Deltares

Enabling Delta Life

Morphological development of the bifurcation at Pannerden

Measurements, simulations and improving of graded-sediment modelling

Deltares

Morphological development of the bifurcation at Pannerden

Measurements, simulations and improving of graded-sediment modelling

11203682-007

Deltares

Title
Morphological development of the bifurcation at Pannerden

Client	Project	Reference	Pages
Rijkswaterstaat Water, Verkeer en Leefomgeving, UTRECHT	11203682-007	11203682-007-ZWS-0005	61

Classification

Keywords
bifurcation, Pannerden, Delft3D, river morphology, sediment transport, trend analysis, coarse immobile layers

Summary
The Pannerden bifurcation is the first bifurcation of the Rhine after it enters the Netherlands. At the bifurcation roughly two thirds of the water is directed westwards towards the Waal and one third heads north towards the Pannerdensch Kanaal. Within the KPP project Versterking Onderzoek Waterveiligheid (strengthening research for water safety) a project was defined to research the redistribution of sediment at the bifurcation. This is an important point in the Netherlands as the distribution of water at the bifurcation is defined by law, and the Dutch government has the task to see to it that this distribution is maintained.

Based on measurements the trends in bed level, transverse bed level in the upstream branch, bed level step over the bifurcation, and grain size were analysed. Next, the Delft3D Rhine branches model was compared to this evolution. The model and and the measurements were from two different periods, making a direct comparison challenging. It seems that the model overestimates the degradation at the bifurcation, as the Boven-Rijn and Pannerdensch Kanaal appear to stabilize in the recently measured bed levels. The trends in grain size development could not be compared as the grain size data were too uncertain. Based on measurements and the model, we conclude that the Waal will continue to deepen compared to the Boven-Rijn, with an increase in discharge towards the Waal. Next the sensitivity of the model to various parameters governing the transverse bed slope in the Boven-Rijn was checked, indicating there are still model parameters which can be used to improve bed level evolution of the model. A simple function relating current upstream grain sizes, upstream transverse slope and bed level steps to future bed level steps at the bifurcation could not be derived.

As the formation and breaking up of coarse immobile layers could play an important role at the bifurcation, particularly in the Pannerdensch kanaal, further research was defined related to the modelling thereof and the implications for sediment management in the rivers. In this regard, a former research code for the modelling of semi-fixed layers was merged with Delft3D-4-DVR, reproducing earlier simplified test cases. These results were analysed in further detail, revealing the neccesity for a model which accurately captures the thickness of the active layer and the partial sediment transport over coarse layers well, as well as sorting mechanisms for the transfer of coarse immobile sediment to the underlayers. Using the combined code a simulation was set up using a constant active-layer thickness, for both the case with and without the semi-fixed layer functionality. The model including this functionality was unstable, crashing after two years of simulation.

Finally, recommendations for further research are presented to be able to model the stabilisation of the Pannerden bifurcation in the future. These include research questions for the improvement of the active-layer model and improvements for the modelling of the bed level evolution in the Rhine branches.

References

Version	Date	Author	Initials	Review	Initials	Approval	Initials
0.1	nov. 2019	Willem Ottevanger Victor Chavarrias		Erik Mosselman		Johan Boon	
1.0	dee. 2019	Victor Chavarrias Willem Ottevanger		Erik Mosselman		Gerard Blom	

Status
final

Deltares

Contents

List of Tables

1 Introduction

The Pannerden bifurcation is the first bifurcation of the Rhine after it enters the Netherlands. At the bifurcation, roughly two thirds of the water is directed westwards towards the Waal and one third heads north towards the Pannerdensch Kanaal. Within the KPP project Versterking Onderzoek Waterveiligheid (strengthening research for water safety) a project is defined to research the redistribution of sediment at the bifurcation. This is an important point in the Netherlands as the distribution of water at the bifurcation is defined by law, and the Dutch government has the task to maintain this water distribution.

Within the project the following research questions are defined related to the morphological evolution at the bifurcation:

1 What is the past morphological development of the Pannerden bifurcation (Chapter 2)?
2 How do the results of the Delft3D DVR model compare to these developments (Chapter 3)?
3 How sensitive is the evolution of the model with respect to the variation of the model inputs related to sorting mechanisms in the BovenRijn (Chapter 4)?
4 How accurate is a simplified predictive function for the evolution of the bed level (Chapter 5)?

As the formation and breaking up of armoured layers could play an important role at the bifurcation, particularly in the Pannerdensch Kanaal, further research was defined related to the modelling thereof and the implications for sediment management in the rivers. Within this context the following additional research questions are defined:

1 How well can the formation and breaking up of armoured layers be modelled using Delft3D-4-DVR? (Chapter 6)
2 Can coarse sediment nourishments be used to stabilize the bed and the water level at the bifurcation? (Chapter 7)

This project was carried out by Victor Chavarrias, Sanjay Giri and Willem Ottevanger. During the project Erik Mosselman had the role of reviewer. We thank Kees Sloff and Erik Mosselman for their input in the discussions about the different modelling concepts for graded sediment. The counterparts from Rijkswaterstaat were Rien van Zetten and Arjan Sieben.

2 Past development of Pannerden bifurcation

2.1 Available data

We have analysed data of bed elevation and grain size distribution. The bed elevation data extend since the beginning of the twentieth century. Until 1999, longitudinal profiles along the river axis and left and right sides where regularly taken. After 1999, multi-beam echosounder data are available. The data were externally preprocessed following the PMAP procedure. The data we received provide mean bed elevation averaged every 100 m for the whole cross-section and discretised between the left and right sections.

The first grain size distribution measurement we have available is in 1956. Measurements are scattered in space (every 1 km) and time (every 8 year in average). Measurement data exist along the left, centre, and right hand sides. The only parameter available in all measurements is the d_{50} of the sediment mixture. For this reason, we focus on this variable. The samples have been taken following different methods. For instance, the measurements in 2000 come from bores, while after that year Rijkswaterstaat used Van Veen grabbers.

The data are available in different formats. The first step has been to combine all available data in one single MATLAB variable that we subsequently use to generate the figures.

2.2 Bed elevation

In this section we analyse longitudinal profiles of bed elevation for the Niederrhein, Boven-Rijn, Pannerdensch Kanaal, and Waal branches. Figure 2.1 shows the bed elevation along the Niederrhein since 1934. The degradational trend is visible. The same trend is better seen when bed elevation is presented relative to 1934 (Figure 2.2). Only in very specific points the current bed level is higher than it was in the past.

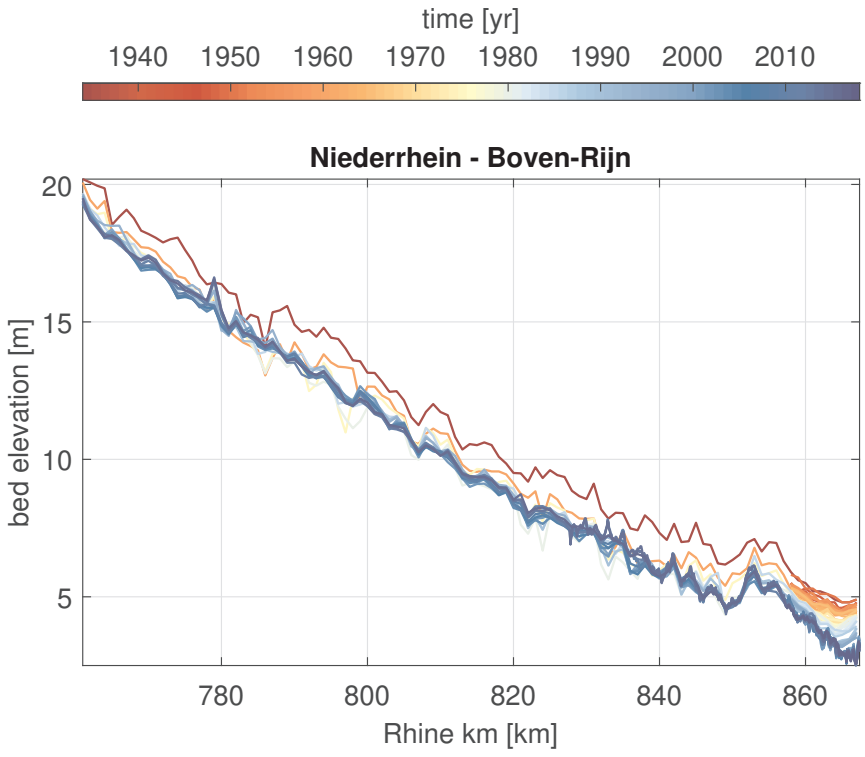

Figure 2.1: *Bed elevation profile of the Niederrhein - Boven-Rijn since 1934*

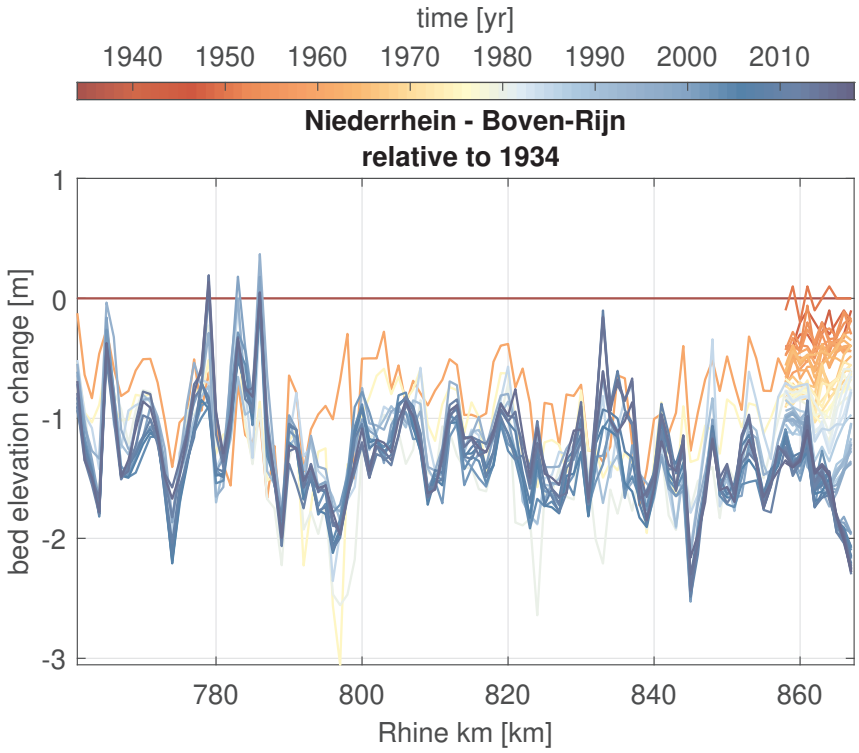

Figure 2.2: *Bed elevation profile of the Niederrhein - Boven-Rijn relative to 1934*

As we are interested in the bifurcation area, we focus on the Boven-Rijn (Figures 2.3 and 2.4). Moreover, we consider the data consistently taken using multi-beam echosounders. The most upstream and downstream sections of the Boven-Rijn may have degraded, but not the central section. Overall, the river has not degraded significantly in the last 20 years. The effect of the sediment nourishment is not striking. Moreover, the effect of the nourishment is not felt right in the bifurcation area, where the river presents a degradational trend.

The Pannerdensch Kanaal has degraded approximately 3 m during the last century (Figures 2.5 and 2.6. Nevertheless, the trend seems to have slowed down for the last decades.

Degradation of the Waal River has not been the same for the whole river (Figures 2.7 and 2.8). The relative data are plotted since 1950, as this is the moment in which the entire river started to be measured. While the upstream part has degraded close to 2 m in the last 70 years, the downstream section has degraded less than 0.5 m.

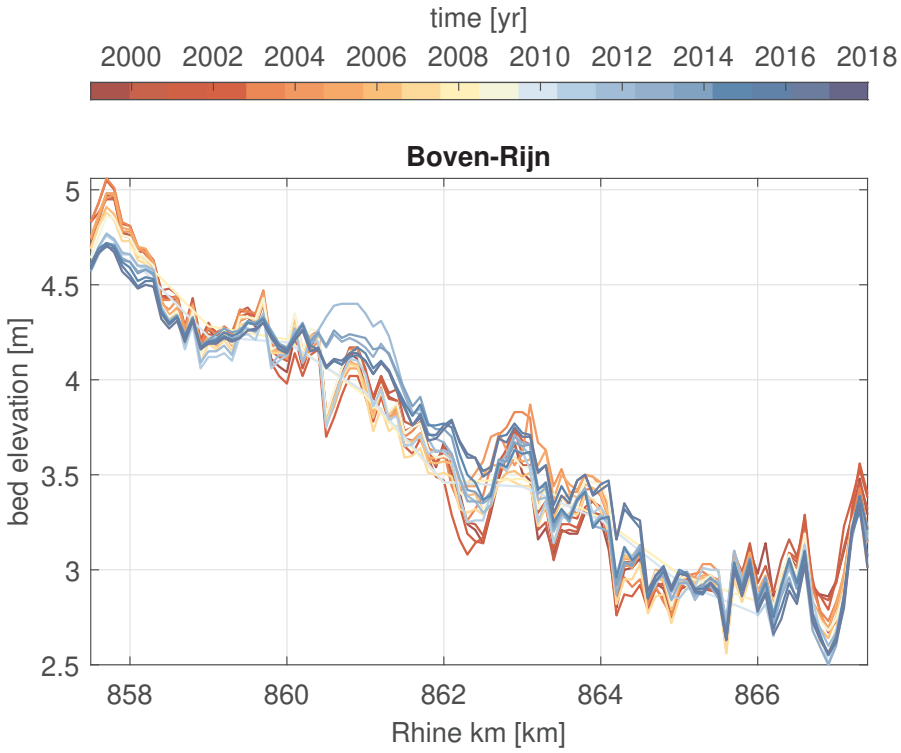

Figure 2.3: *Bed elevation profile of the Boven-Rijn since 1999*

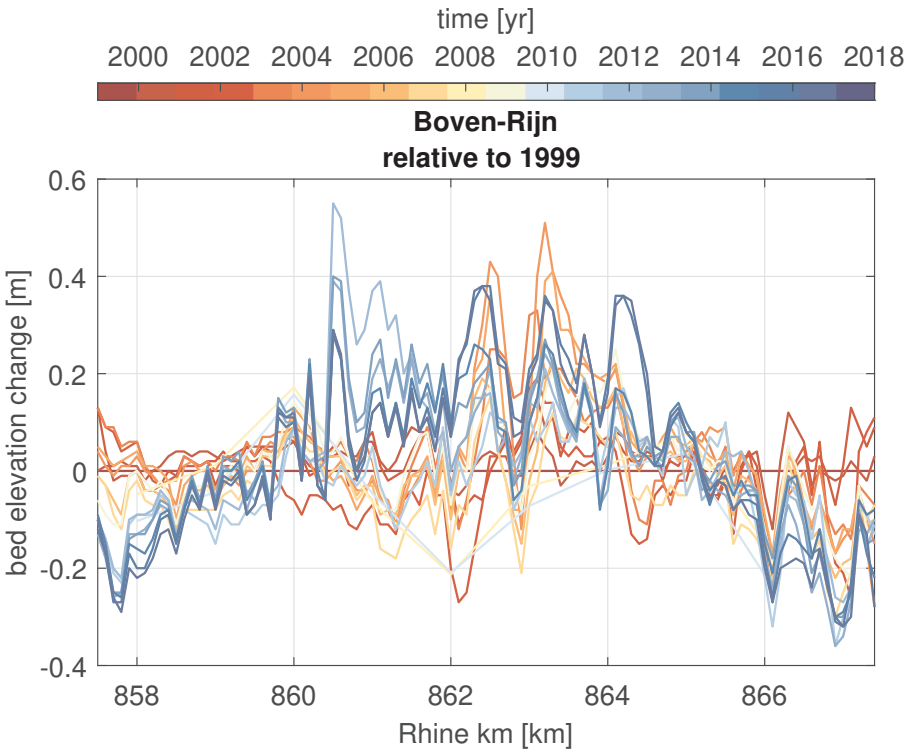

Figure 2.4: *Bed elevation profile of the Boven-Rijn relative to 1999*

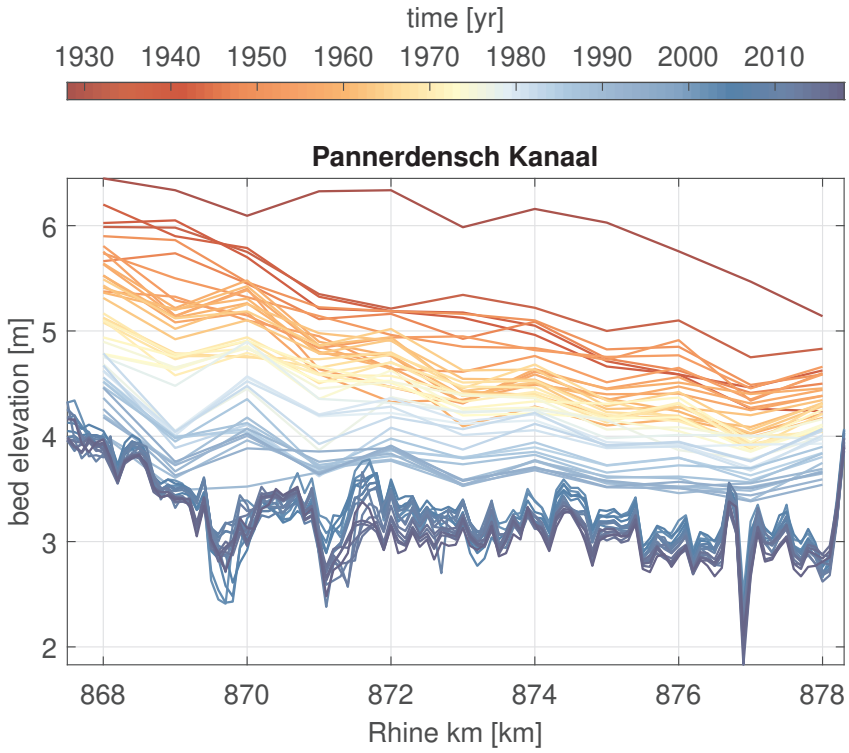

Figure 2.5: *Bed elevation profile of the Pannerdensch Kanaal since 1926*

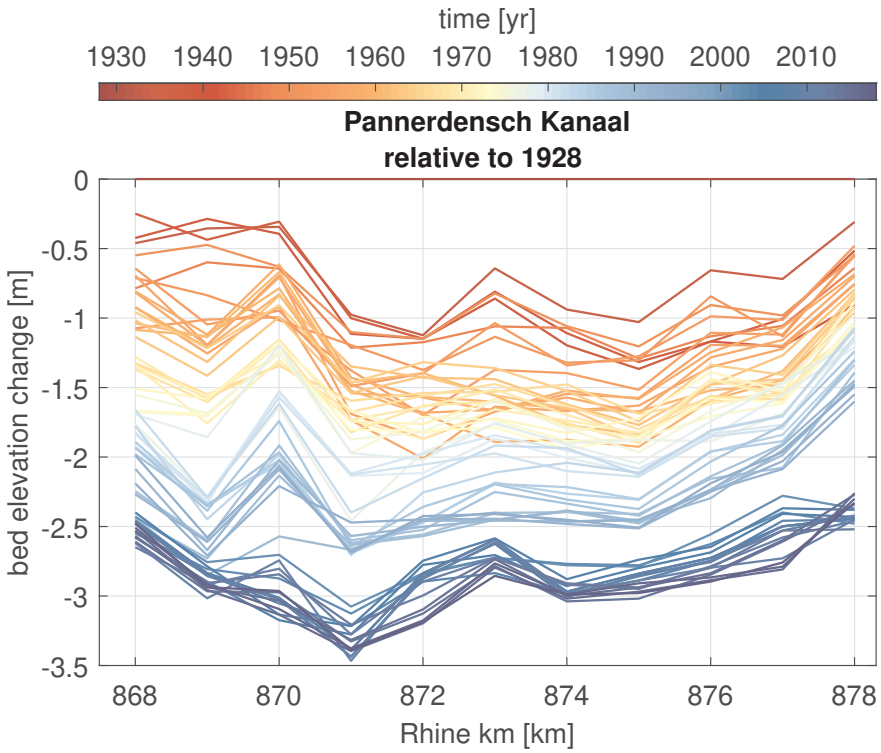

Figure 2.6: *Bed elevation profile of the Pannerdensch Kanaal relative to 1926*

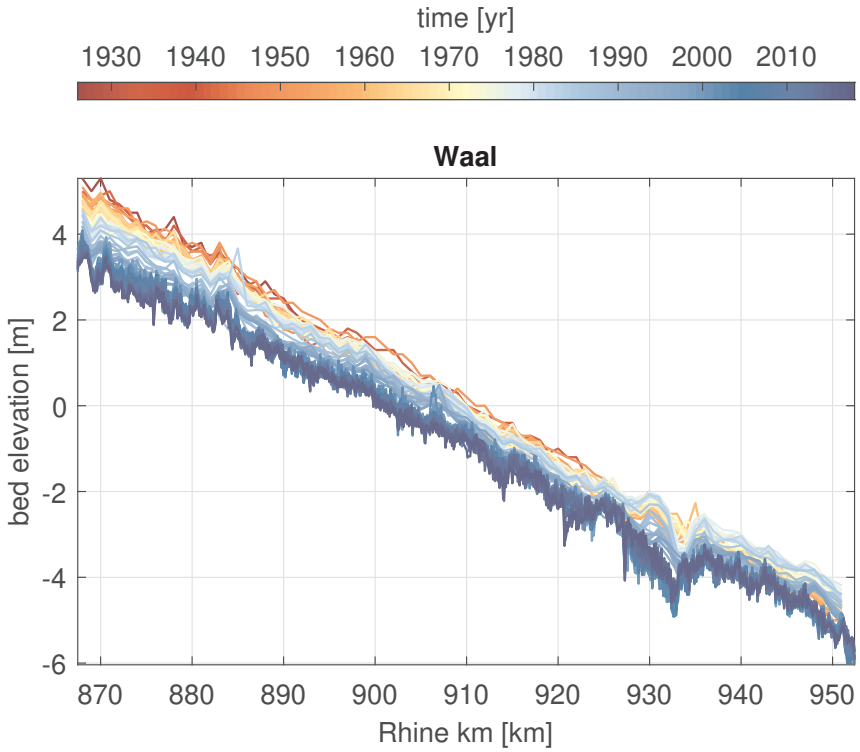

Figure 2.7: *Bed elevation profile of the Waal since 1926*

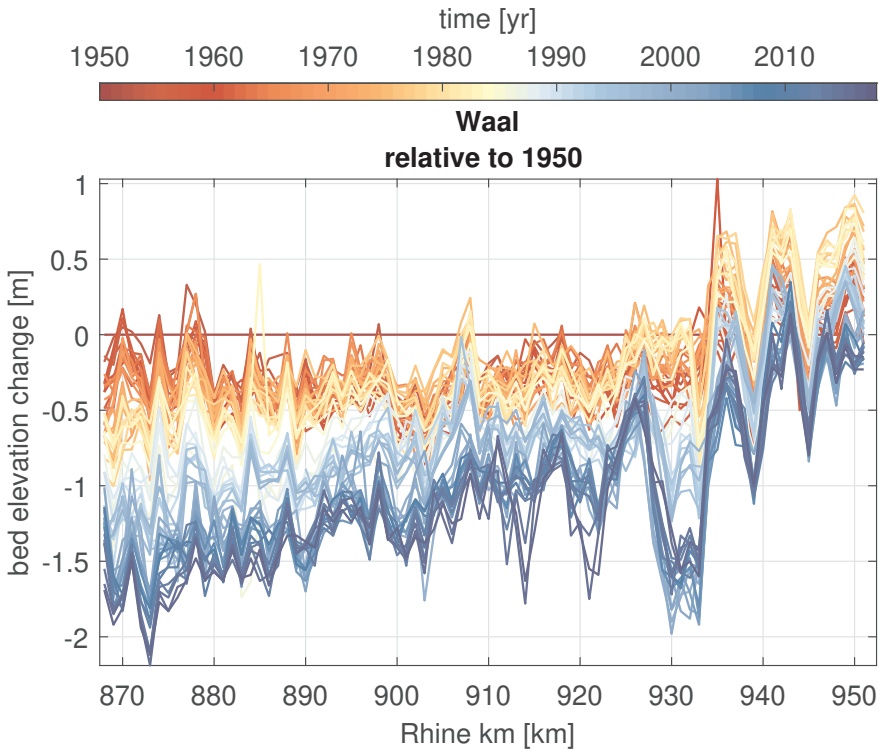

Figure 2.8: *Bed elevation profile of the Waal relative to 1950*

2.3 Transverse bed slope

In this section we focus on the transverse bed slope. To this end, we analyse the bed elevation measurements taken along the left and right hand side. Figures 2.9 and 2.10 show these data for the Niederrhein and the Boven-Rijn, respectively. A possible trend showing a change in transverse bed slope is superimposed to the overall degradational trend, which complicates the analysis of the data. In order to estimate whether there has been a change of the transverse bed slope with time, we compute the absolute value of the difference between the left and right measurements for each time. Subsequently, we fit a first-order polynomial to the absolute difference with time. This allows us to obtain an estimation of the rate of change (Figure 2.11). Values larger than zero indicate that the bed slope has increased and vice versa. From river kilometre 760 until 780, the bed slope of the bends has increased, while it has decreased between 780 and 830, approximately. There are several reasons that explain a decrease of the transverse slope. One is maintenance dredging. As sediment may not be extracted from the river, dredged sediment is dumped at deeper locations. A second explanation is bed surface coarsening, as an increase in the grain size is related to a decrease in the transverse bed slope. The data from kilometre 830 onwards are noisier than in the upstream section. This is because measurements are taken more frequently. This gives an estimation of the accuracy of the method. If the noise would be such that the signal is not visible, the data of the upstream region should be taken with caution, as the trend could be spurious. We observe that some bends have increased the bed slope, but the ones closer to the bifurcation have decreased the slope.

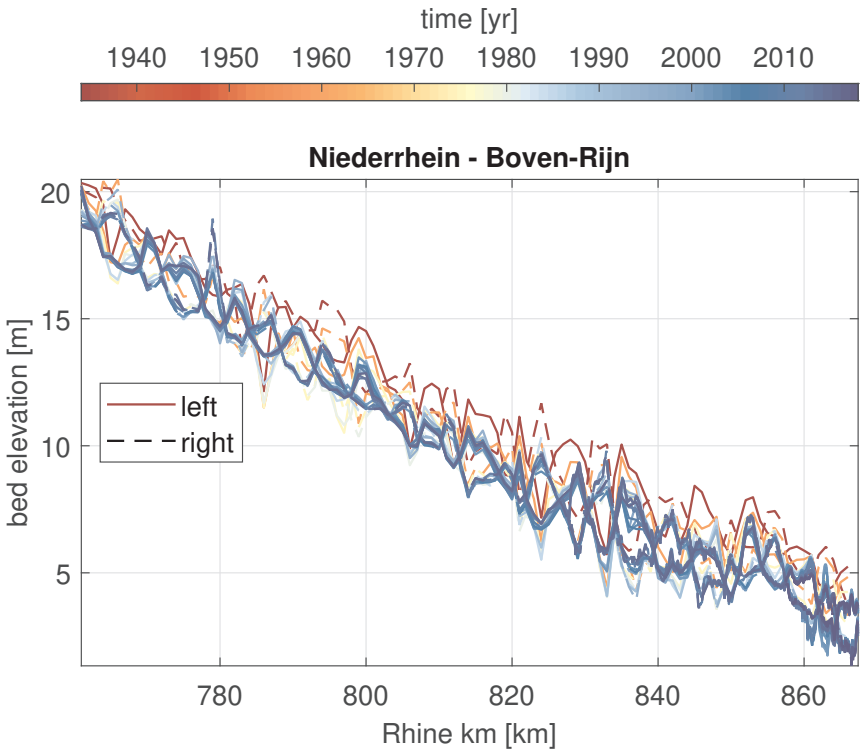

Figure 2.9: *Left and right bed elevation profile of the Niederrhein - Boven-Rijn.*

Along the Pannerdensch Kanaal, the trend is that the transverse bed slope increases (Figures 2.12 and 2.13), while along the Waal River, the trend is opposite (Figures 2.14 and 2.15), especially along the upstream section (Figure 2.14).

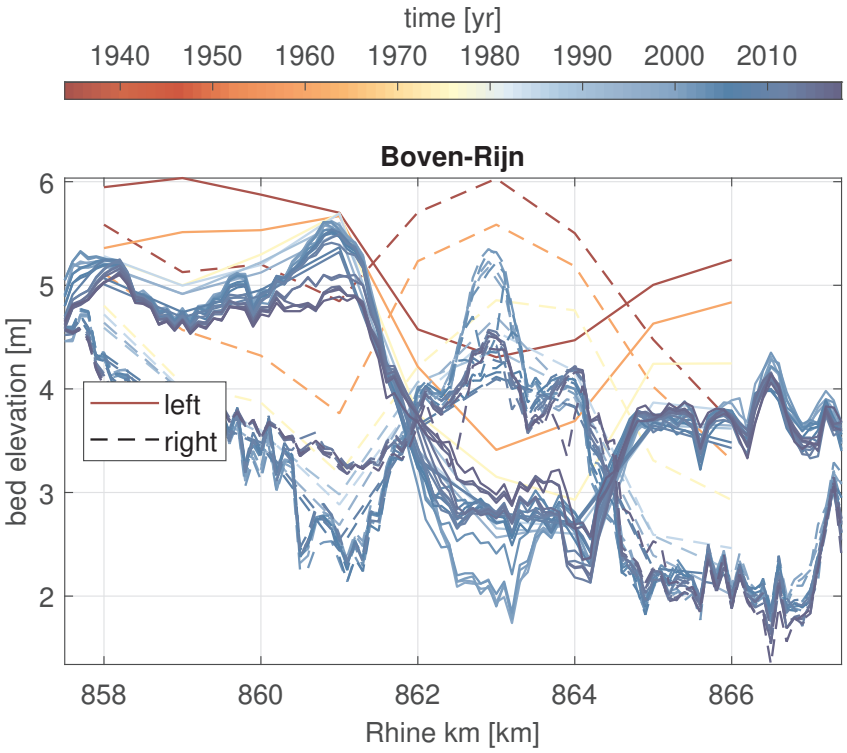

Figure 2.10: *Left and right bed elevation profile of the Boven-Rijn.*

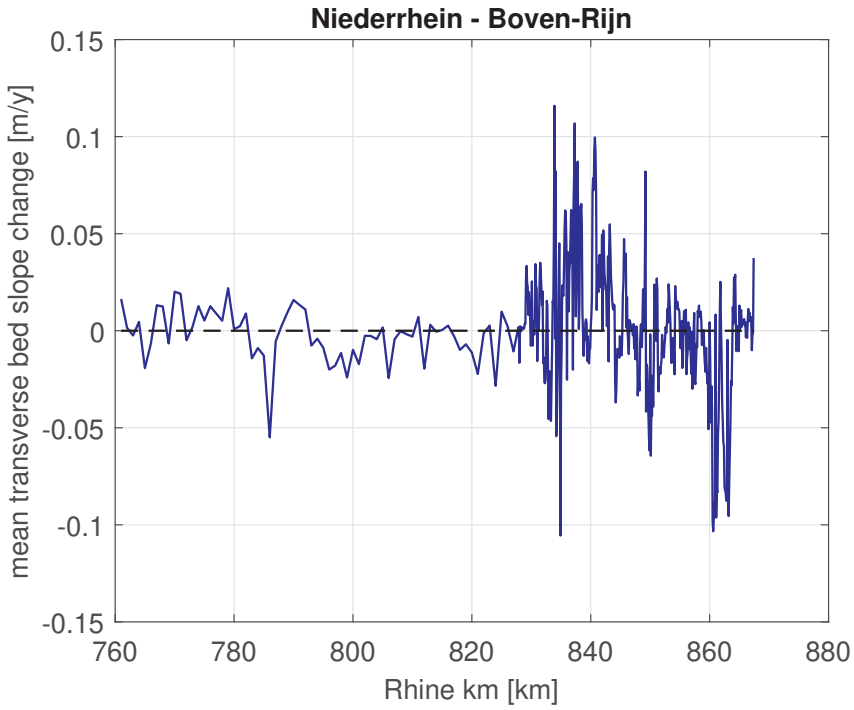

Figure 2.11: *Mean change with time of the absolute difference between left and right bed elevation. A positive (negative) value indicates increase (decrease) in the transverse bed slope.*

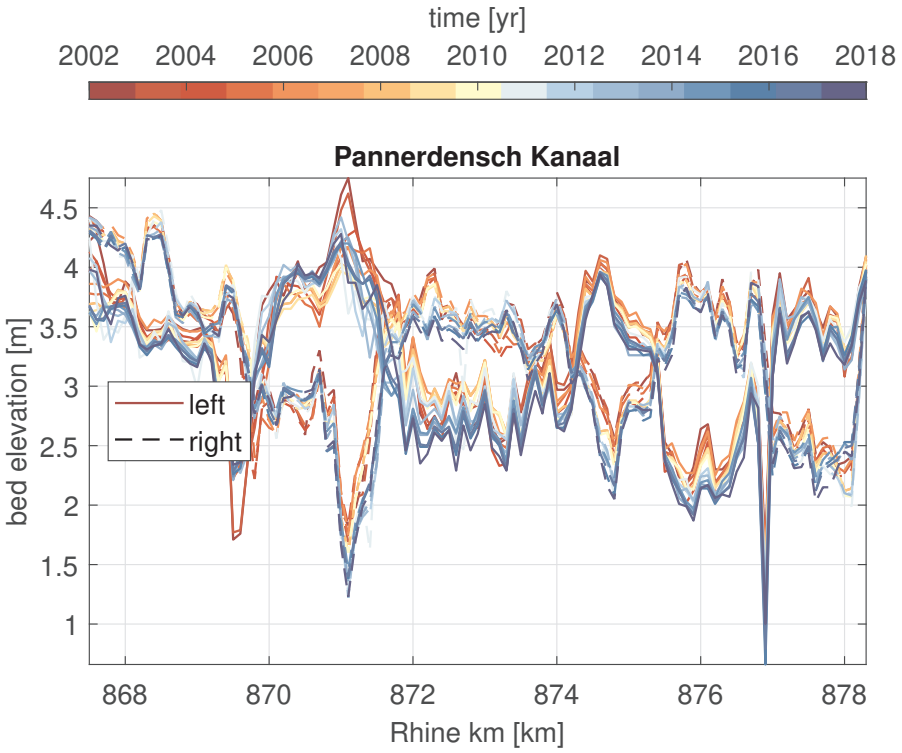

Figure 2.12: *Left and right bed elevation profile of the Pannerdensch Kanaal.*

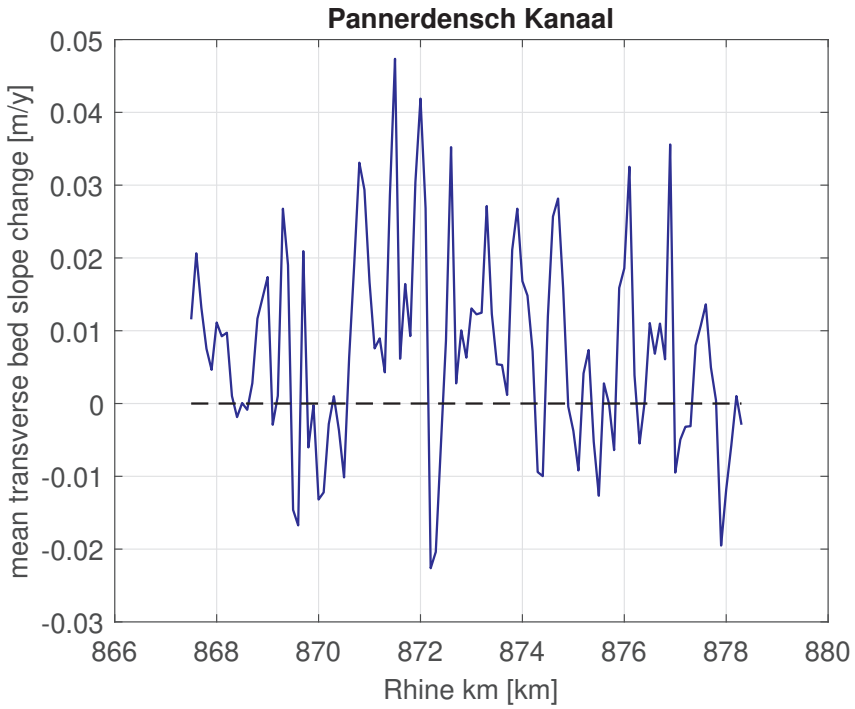

Figure 2.13: *Mean change with time of the absolute difference between left and right bed elevation. A positive (negative) value indicates increase (decrease) in the transverse bed slope.*

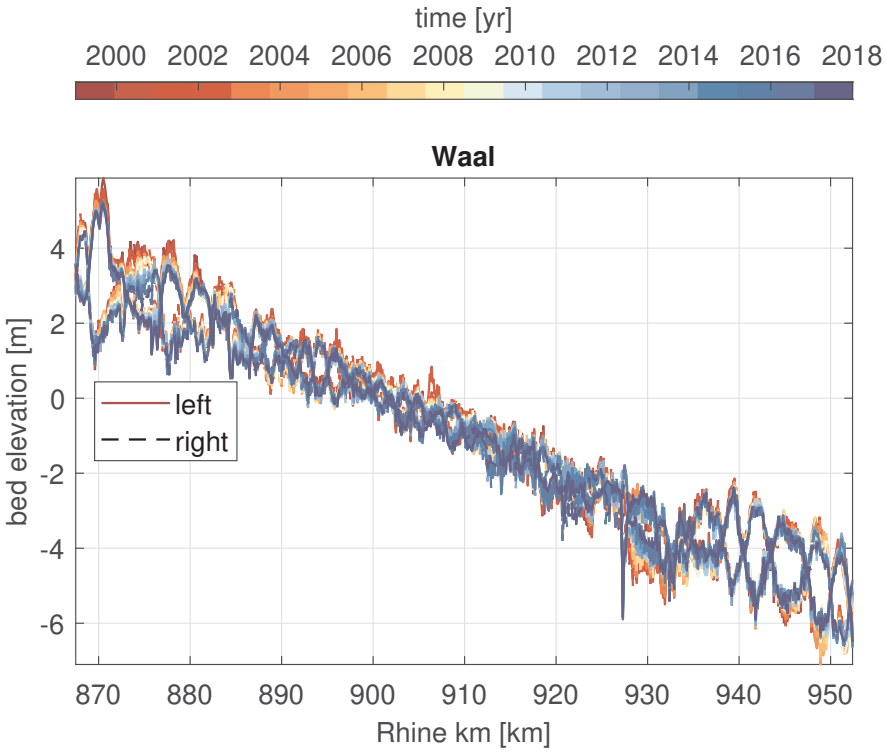

Figure 2.14: *Left and right bed elevation profile of the Waal.*

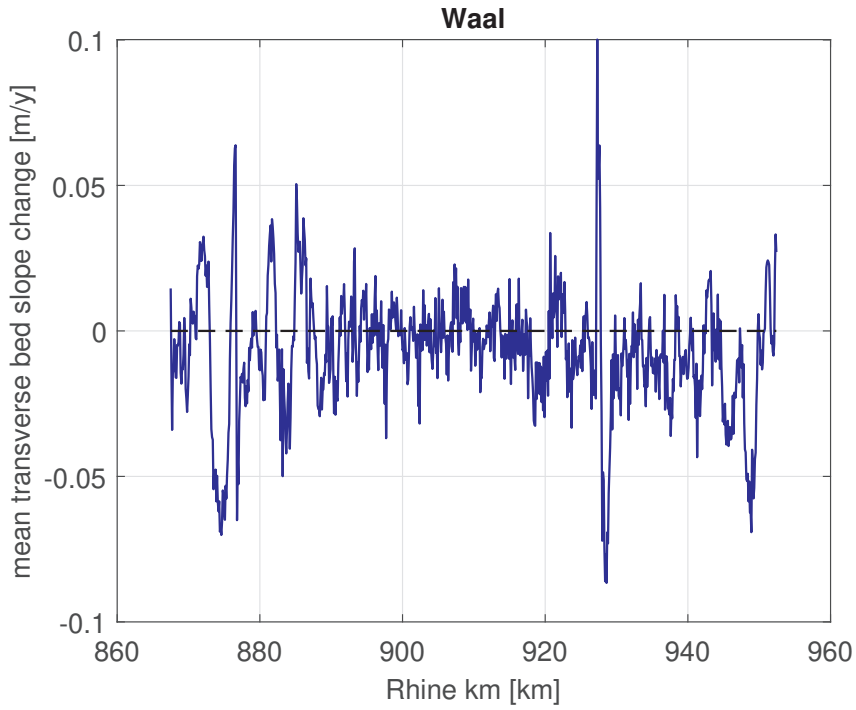

Figure 2.15: *Mean change with time of the absolute difference between left and right bed elevation. A positive (negative) value indicates increase (decrease) in the transverse bed slope.*

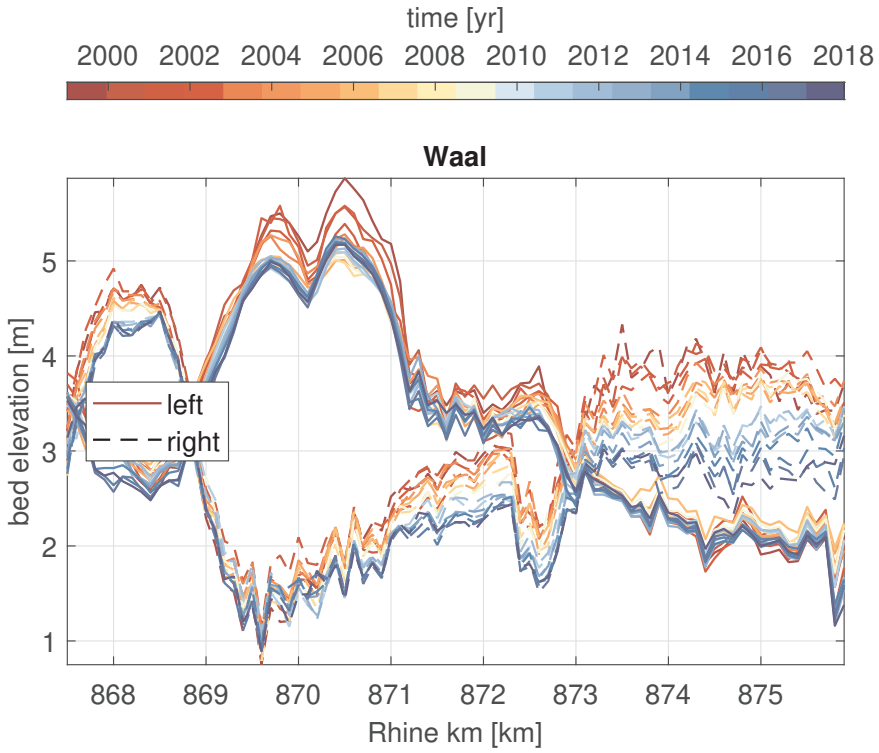

Figure 2.16: *Left and right bed elevation profile of the Waal (upstream section).*

2.4 Bed level step

In this section, we focus on the bed level step occurring at the bifurcation area. Figure 2.17 shows the bed elevation with time along the last 2 km of the Boven-Rijn and first 2 km of the Pannerdensch Kanaal. Figure 2.18 shows the same information along the Boven-Rijn - Waal branch. Note that the density of the data change after the multibeam echosounder is introduced. We compute the mean elevation at each time (Figure 2.19). We observe the overall degradational trend for all branches. The bed elevation of the upstream end of the Waal is always higher than the bed elevation of the downstream end of the Boven-Rijn. However, until 1999 the difference is small. There is a sudden change which is difficult to explain from a physical process occurring in the river. It might be explained by the change in measurement procedure from singlebeam to multibeam. The area covered by the multibeam measurements may include lower areas of the cross section previously ignored. From 1999 onwards, the degradation rates of the downstream end of the Boven-Rijn and the upstream end of the Pannerdensch Kanaal seem to decrease, while the upstream section of the Waal continues degrading at a similar rate as previously observed. This comment must be considered with caution, as the data set may not be sufficiently long to clearly confirm the observation.

The change with time of the bed level step (downstream value minus the upstream value) is shown in Figures 2.20 and 2.21.

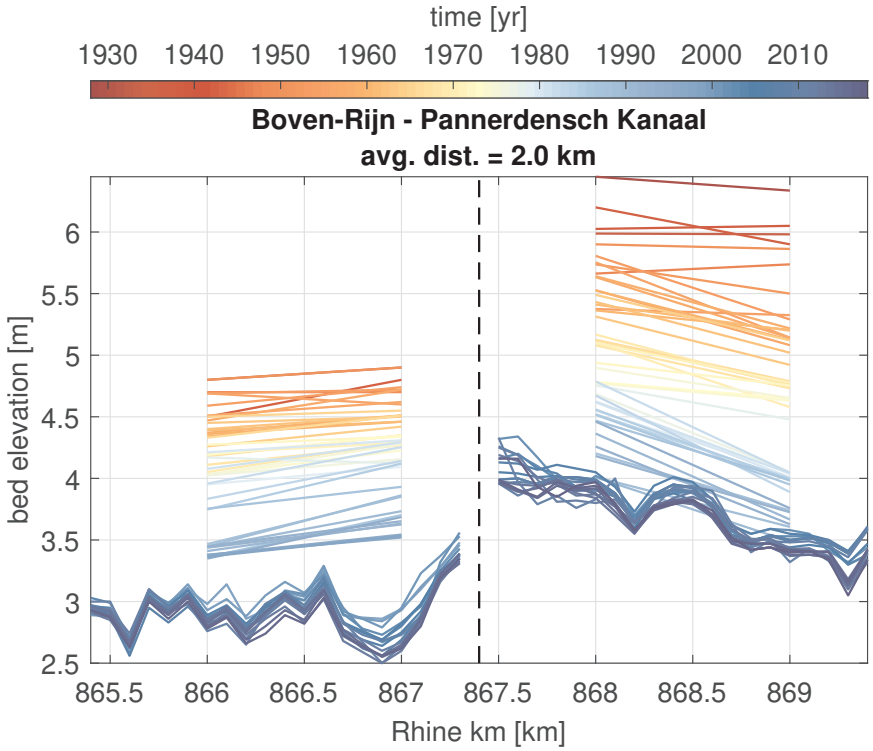

Figure 2.17: *Bed elevation with time 2 km upstream and downstream from the Pannerdensche Kop along the Boven-Rijn and Pannerdensch Kanaal branches.*

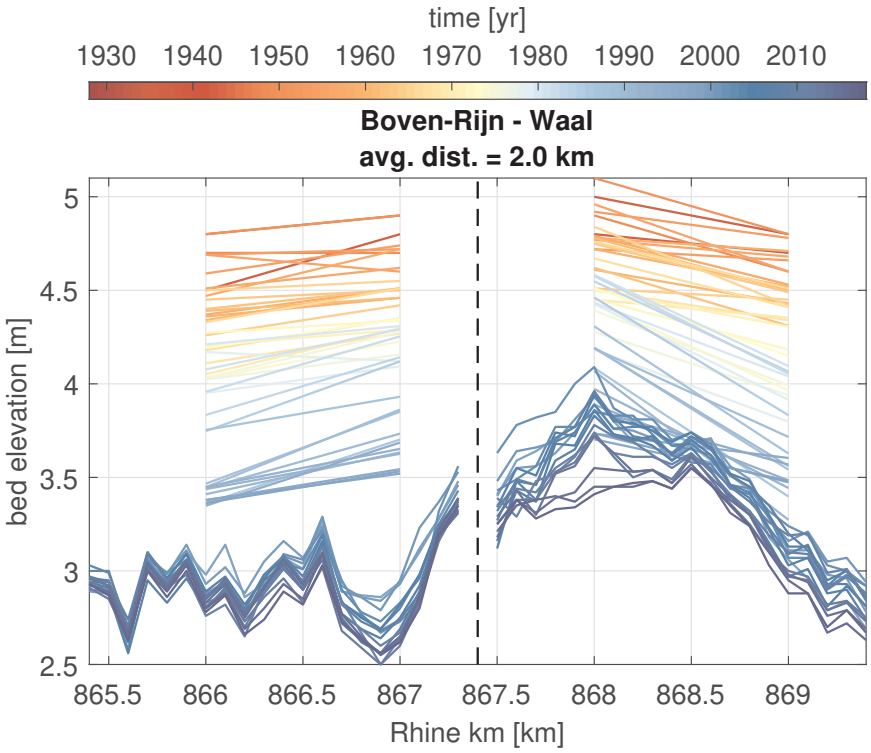

Figure 2.18: *Bed elevation with time 2 km upstream and downstream from the Pannerdensche Kop along the Boven-Rijn and Waal branches.*

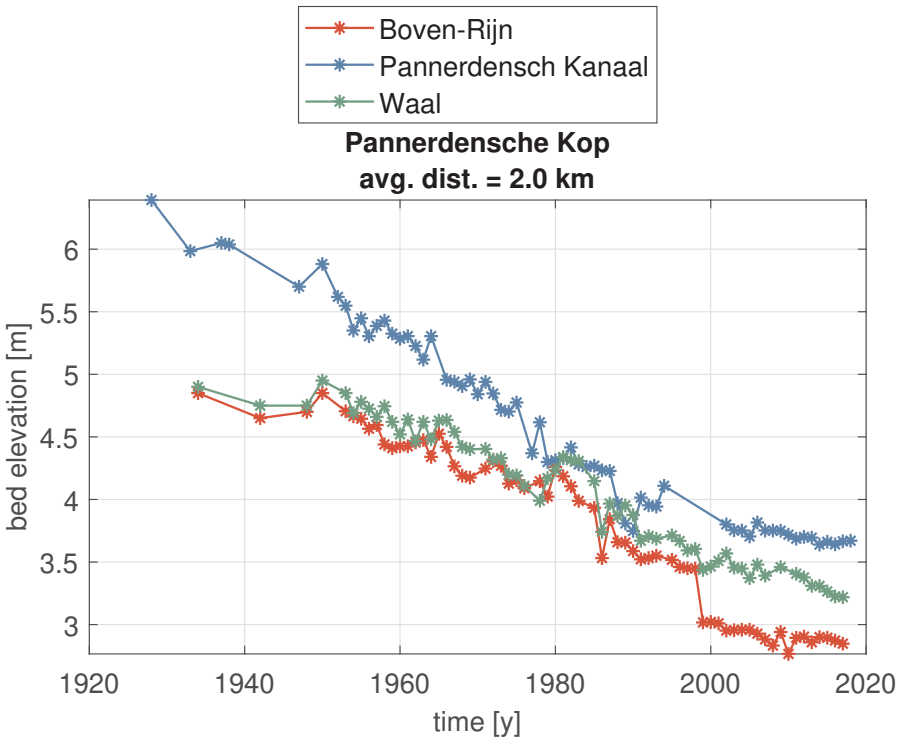

Figure 2.19: *Mean (along 2 km) bed elevation with time for all branches of the Pannerdensche Kop.*

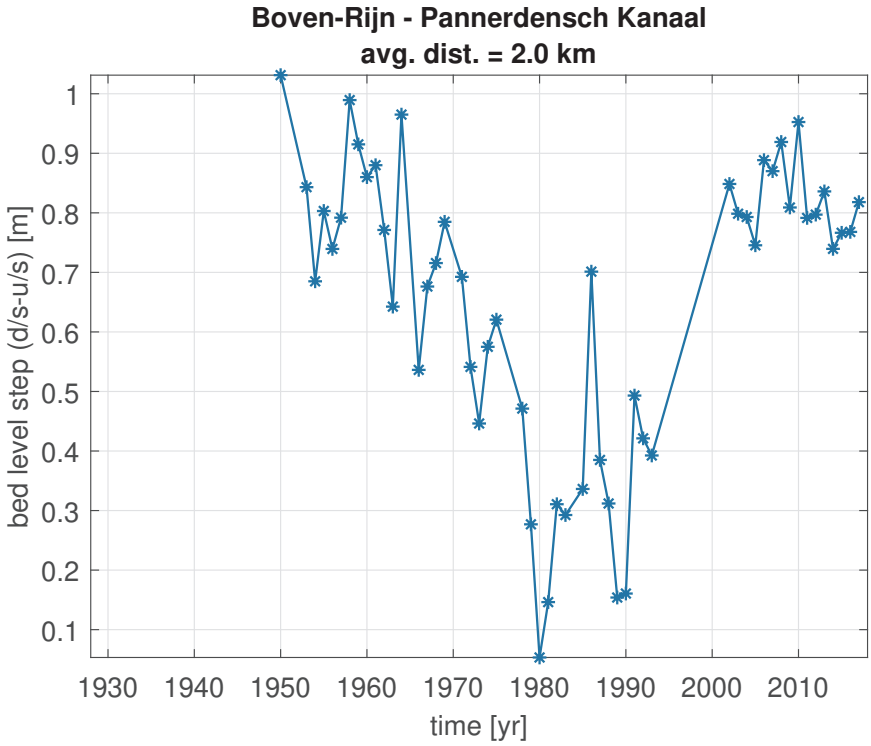

Figure 2.20: *Bed level step at the Pannerdensche Kop along the Boven-Rijn and Pannerdensch Kanaal branches.*

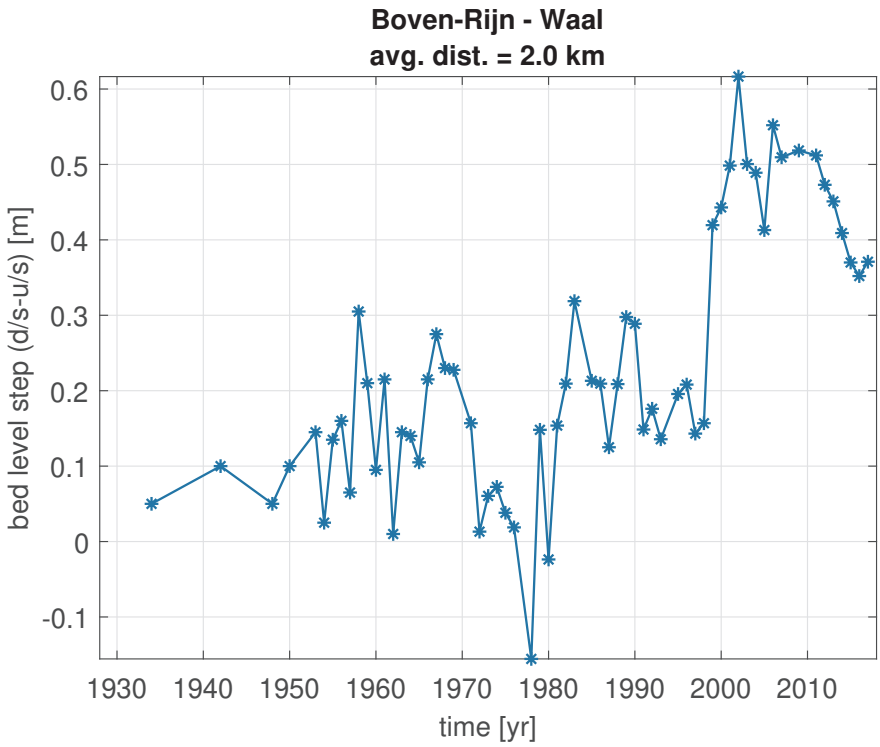

Figure 2.21: *Bed level step at the Pannerdensche Kop along the Boven-Rijn and Waal branches.*

2.5 Grain size

In this section we focus on the grain size distribution of the bed surface. Figure 2.24 presents a longitudinal profile of the d_{50} at the bed surface along the axis of the Boven-Rijn since 1951. The grain size varies between 0.5 mm and 50 mm. This large variation can be understood from several factors. First is the intrinsic variation in surface grain size. For instance, sediment at the crest of a dune is finer than at the trough. The flow stage has an influence too. These variations have length scales smaller than 500 m and temporal scales much smaller than 10 years. For this reason, we find the data set not usable to extract detailed conclusions on coarsening or fining of the river bed. Moreover, we need to consider that the sampling method has not been the same in taking all measurements.

Scatter in grain size data can partly be ascribed to substantial variations in space and time. Bed sediment composition is not uniform but shows patches of coarser and finer sediments (cf. Paola and Seal (1995) and Figure 2.22). Sampling at two different locations in the same area may hence lead to different results. Furthermore, coarse layers forming in the troughs of dunes during floods may still be exposed shortly after a flood but become buried under finer sediment with the passing of time (cf. Figure 2.23). Sampling at the same location at different points of time can hence produce different results too. Moreover, sampling with a lower frequency than the frequency at which variations in bed sediment composition occur carries the risk of identifying spurious trends due to aliasing. This calls for caution in the analysis and interpretation of measurement data.

Figure 2.22: *Coarser and finer sediment on the bed of the Boven-Rijn (photo Erik Mosselman, 19 April 2011).*

We attempt to understand whether the bed surface has become coarser or finer with time. To this end, we plot the grain size at each cross section with time (Figure 2.25). The colour indicates the river kilometre. Lines unite samples taken at the same location at different times. No conclusive information can be extracted from this information. The samples taken in 2008 may be slightly coarser than previous samples. However, given the data scatter, this can not be confirmed. Figure 2.26 presents the same information is a different manner. In this plot, the grain size is relative to the first measurement. We note that variations are of the order of 2 to 4 mm, which is small compared to the expected variability due to sampling frequency.

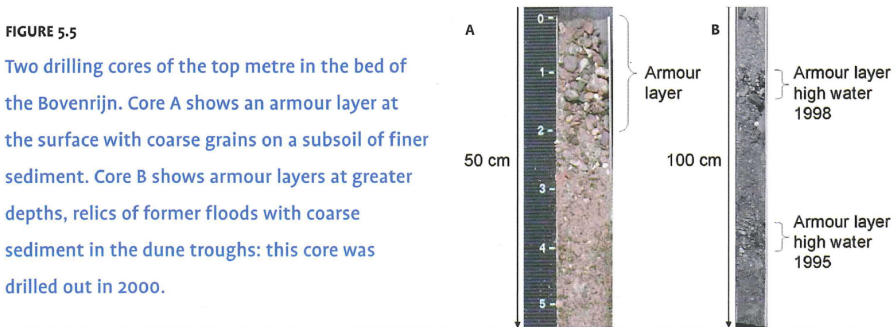

Figure 2.23: *Drilling cores of the top metre in the bed of the Boven-Rijn, showing coarser and finer layers (Ten Brinke, 2005)*

This supports the conclusion that it is not possible to clearly state that the bed surface has significantly changed the grain size distribution.

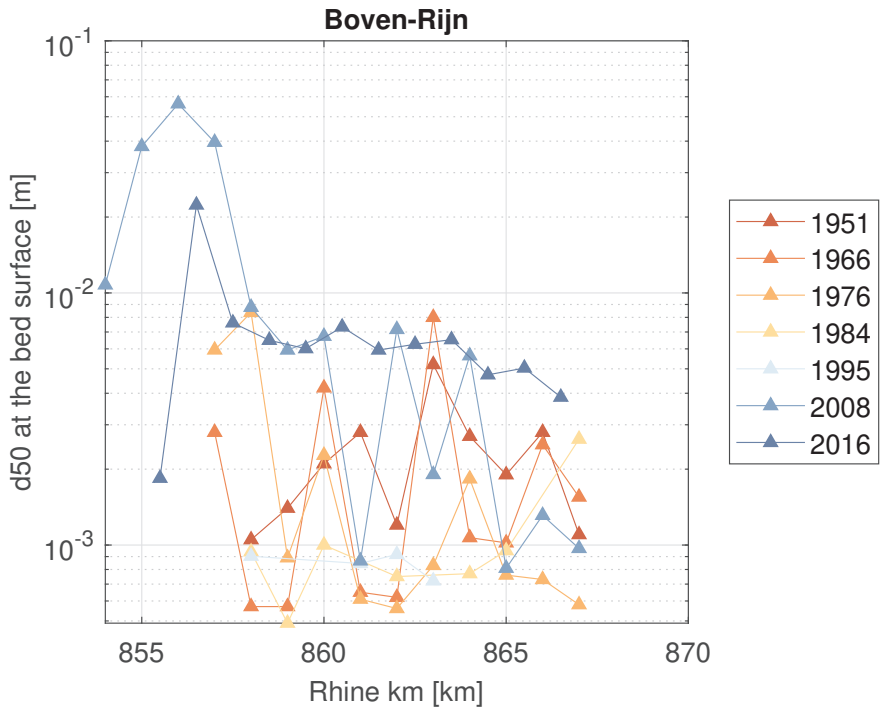

Figure 2.24: *Longitudinal profile along the Boven-Rijn of the d_{50} at the bed surface.*

Figures 2.27, 2.28, and 2.29 present the same information as explained above, but this time for the Pannerdensch Kanaal. The variability is as large as in the Boven-Rijn. Moreover, there are less data available. It is not possible to conclude whether the bed surface has become coarser or finer with time. It is not even possible to conclude whether the Pannerdensch Kanaal is coarser or finer than the Boven-Rijn.

In the case of the upstream section of the Waal River (Figures 2.30, 2.31, and 2.32), it is possible to observe that the bed surface is finer than in the case of the Boven-Rijn. Apart from the most upstream samples, the maximum d_{50} is smaller than 2 mm. Again, one should note that the last profile covering the upstream 10 km of the Waal River available to us was taken a

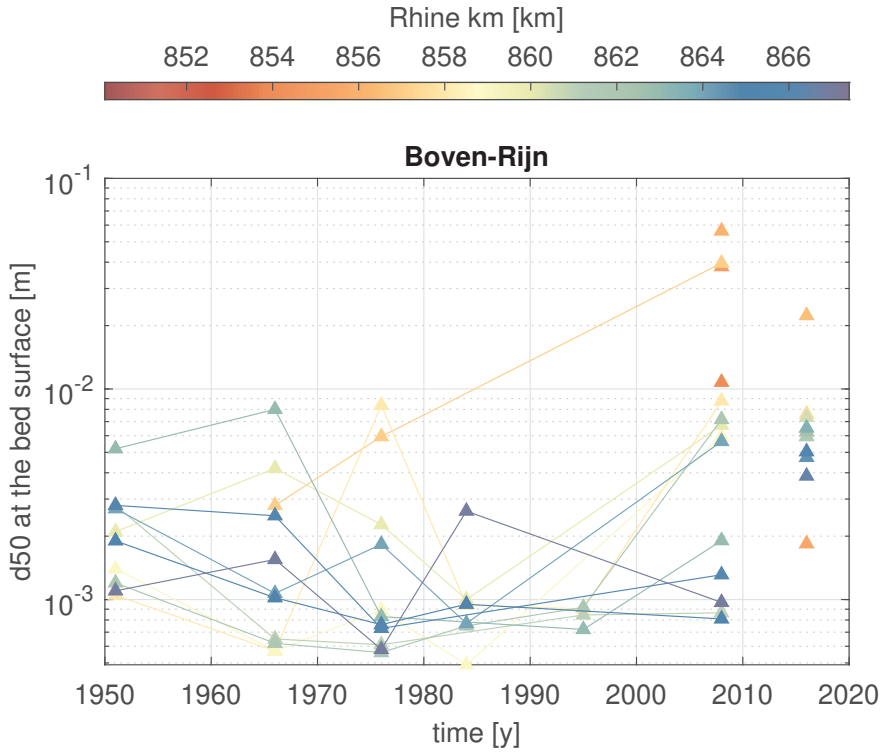

Figure 2.25: *Time evolution along the Boven-Rijn of the d_{50} at the bed surface.*

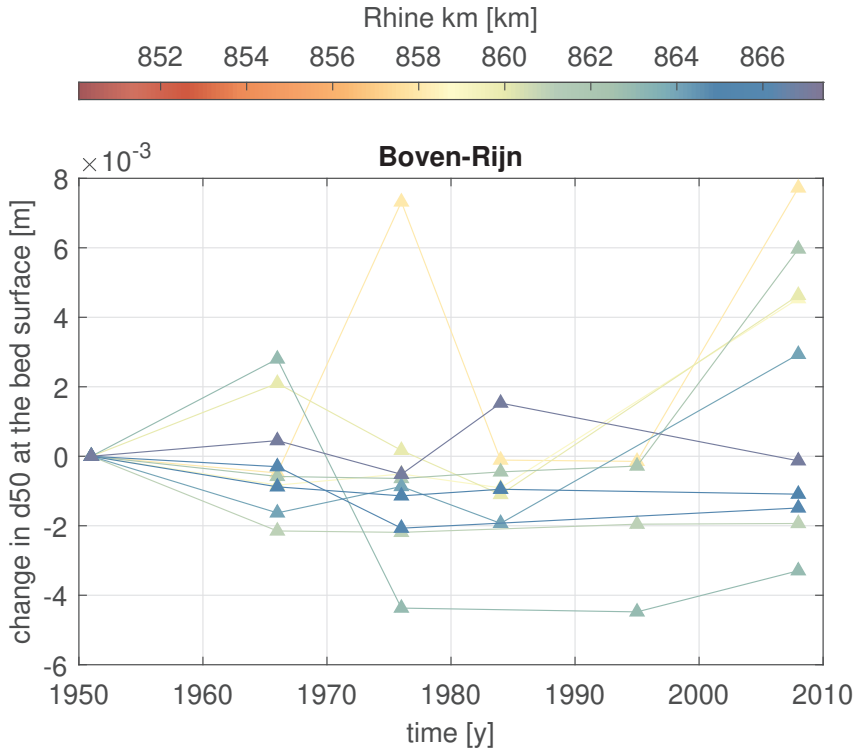

Figure 2.26: *Time evolution along the Boven-Rijn of the d_{50} at the bed surface relative to 1950.*

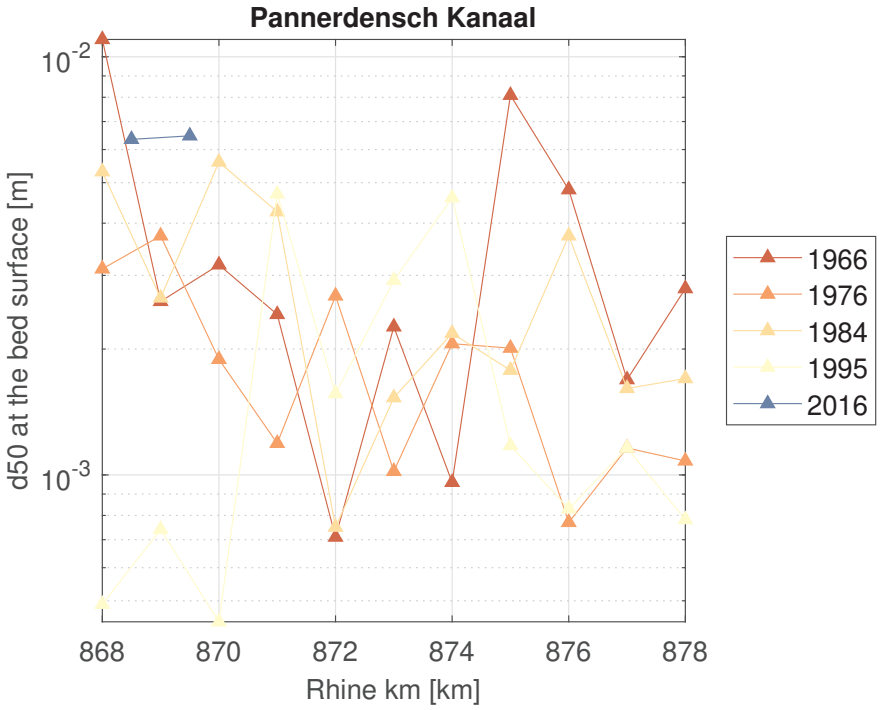

Figure 2.27: *Longitudinal profile along the Pannerdensch Kanaal of the d_{50} at the bed surface.*

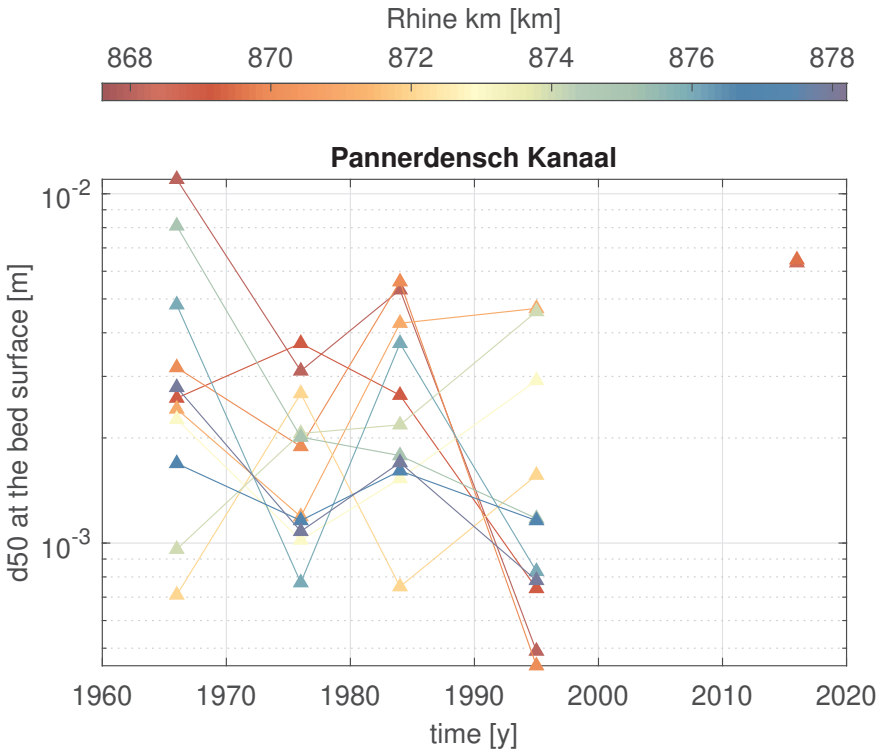

Figure 2.28: *Time evolution along the Pannerdensch Kanaal of the d_{50} at the bed surface.*

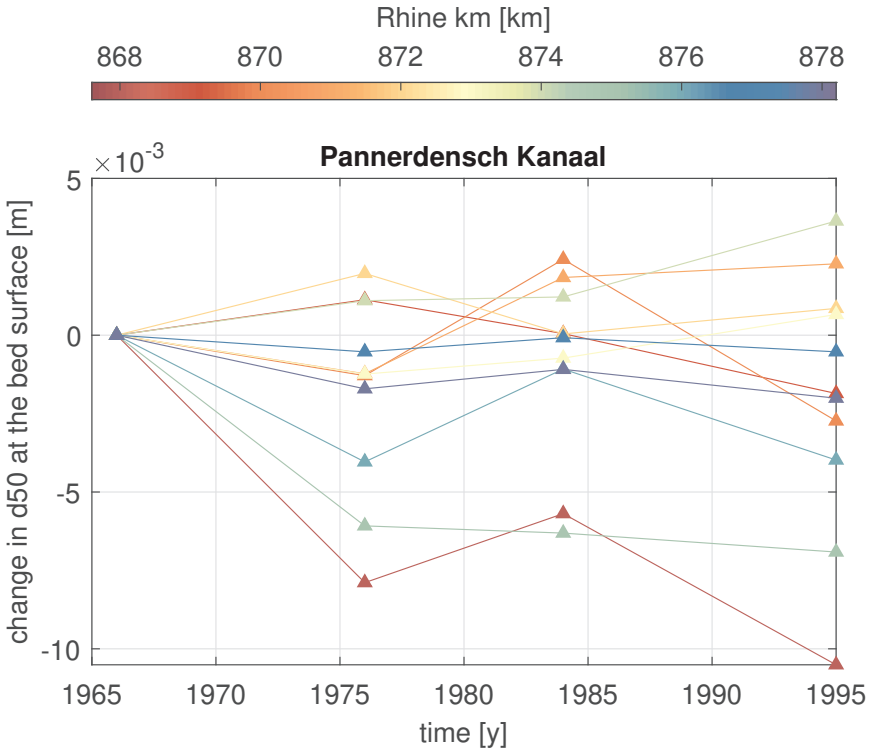

Figure 2.29: *Time evolution along the Pannerdensch Kanaal of the d_{50} at the bed surface relative to 1950.*

quarter of a century ago. The available data are insufficient to conclude grain size distribution changes along the Waal River.

We have considered the data on the river axis only. In Figures 2.33 and 2.34 we present the d_{50} along the left and right sides of the Boven-Rijn, respectively. Similarly to the data along the axis, the scatter is too large to derive strong conclusions. Note how, for instance, the left side of the most upstream section of the Boven-Rijn in 2000 is consistently between 5 mm and 10 mm while the right hand side varies between 0.5 mm and 10 mm. More downstream, the variability is reversed. Focusing on one particular bend, such as the one in front of Spijk (river-kilometre 856 - 861), we may say that the data show that the right-hand side (i.e., the outer bend) is slightly coarser than the left-hand side, as predicted by theory. However, we would expect the opposite pattern in the next bend (i.e, the one in front of Tolkamer, between river-kilometres 861 and 864), and this cannot be seen in the data. We conclude that the data are inconclusive.

Figure 2.35 and 2.36 present the changes with time for each sample on the left and the right, respectively, and Figures 2.37 and 2.38 the grain size relative to the first measurement. We do not observe a significant fining or coarsening pattern.

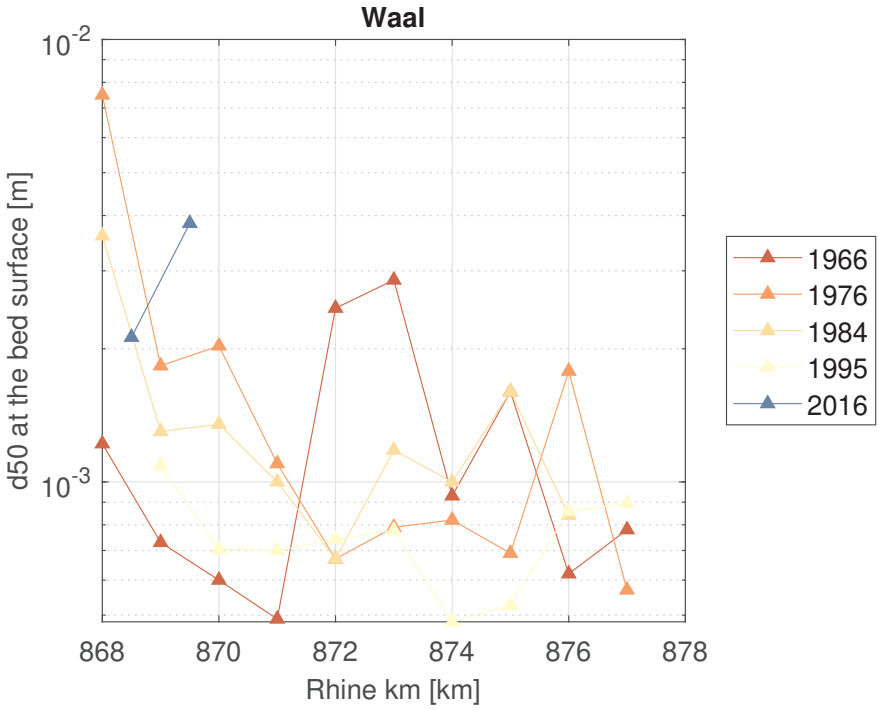

Figure 2.30: *Longitudinal profile along the Waal of the d_{50} at the bed surface.*

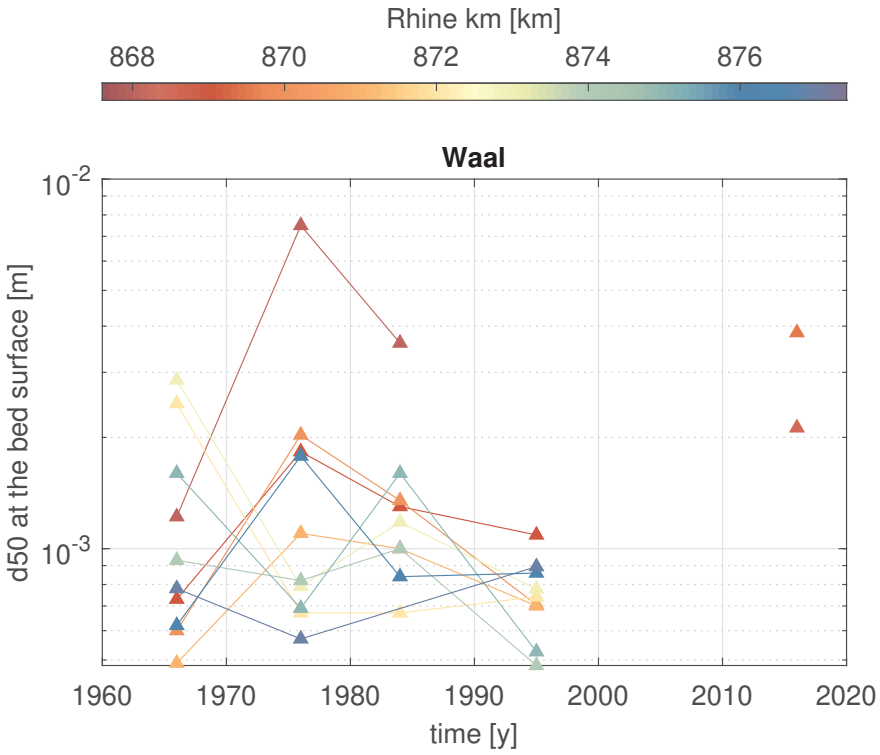

Figure 2.31: *Time evolution along the Waal of the d_{50} at the bed surface.*

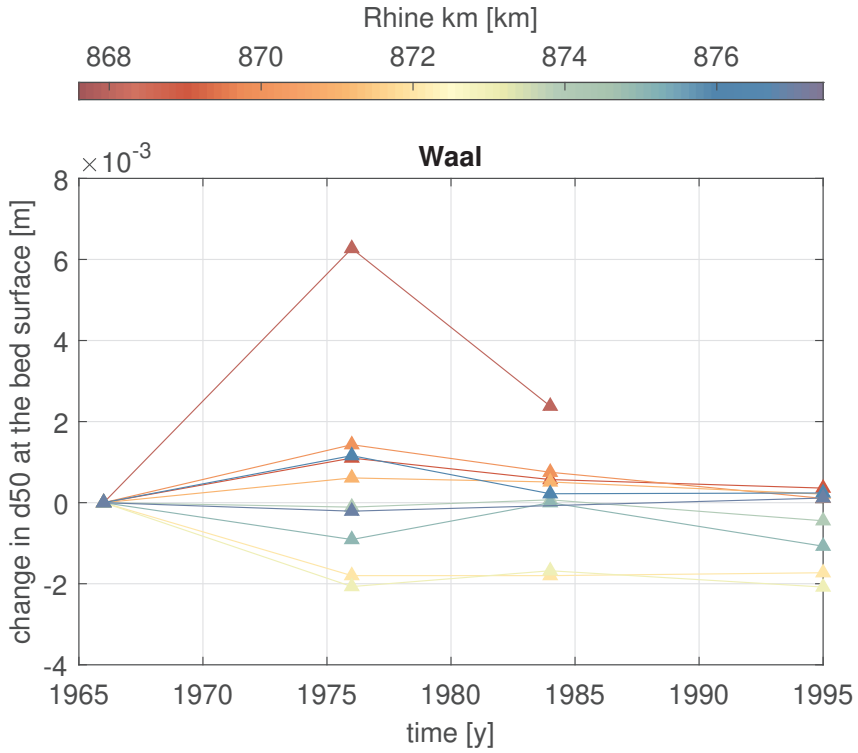

Figure 2.32: *Time evolution along the Waal of the d_{50} at the bed surface relative to 1950.*

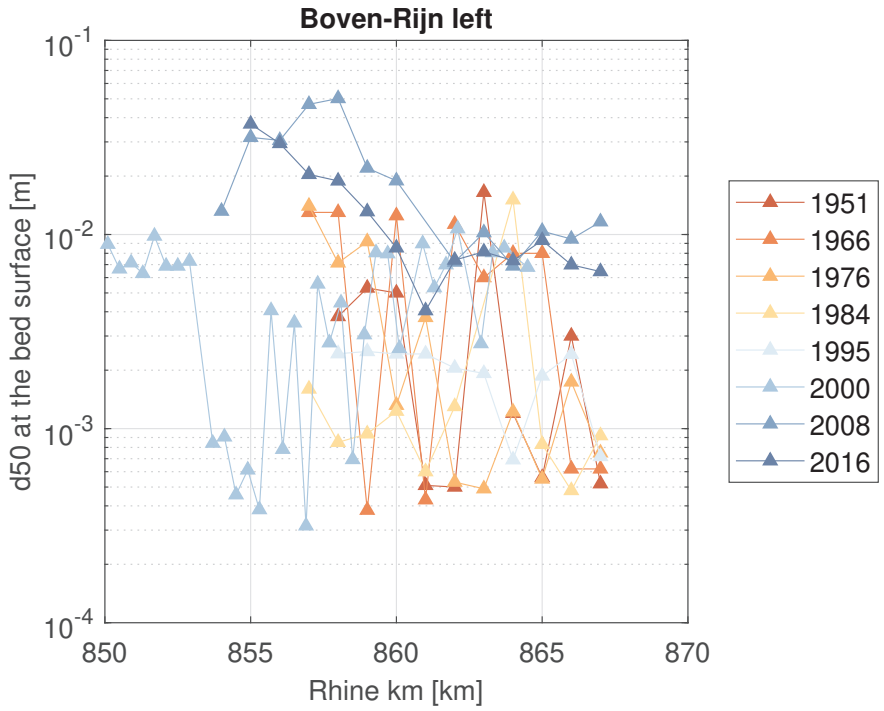

Figure 2.33: *Longitudinal profile of the d_{50} at the bed surface along the left side of the Boven-Rijn.*

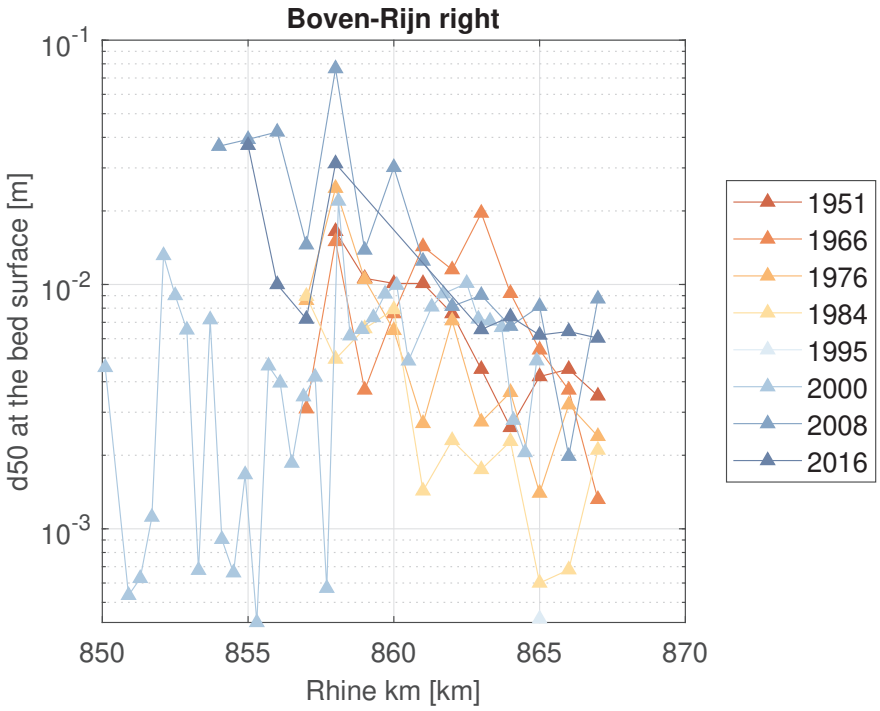

Figure 2.34: *Longitudinal profile of the d_{50} at the bed surface along the right side of the Boven-Rijn.*

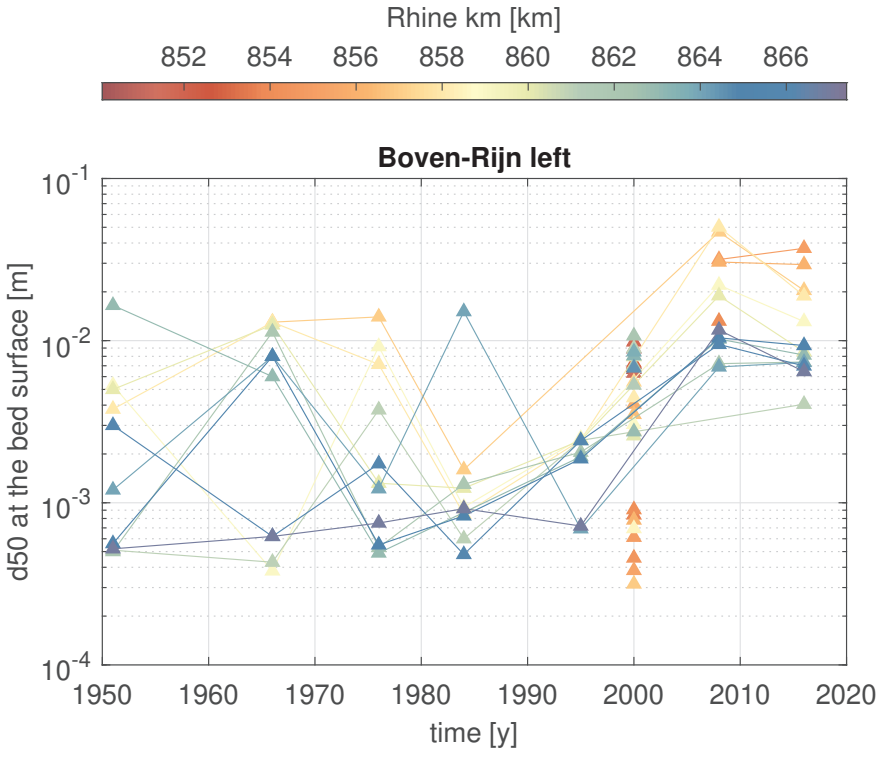

Figure 2.35: *Time evolution of the d_{50} at the bed surface along the left side of the Boven-Rijn.*

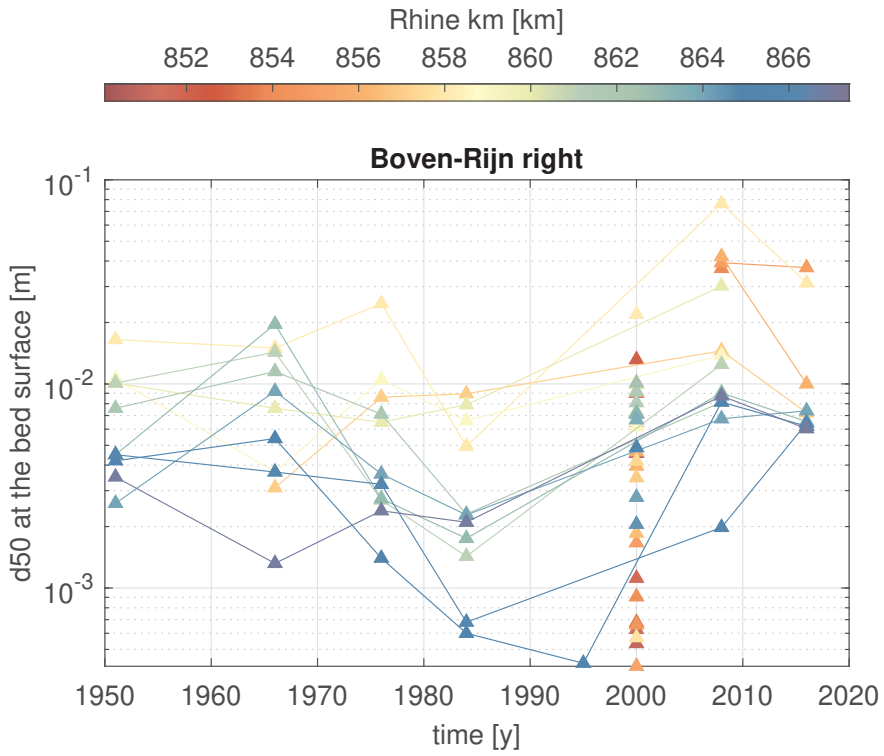

Figure 2.36: *Time evolution of the d_{50} at the bed surface along the right side of the Boven-Rijn.*

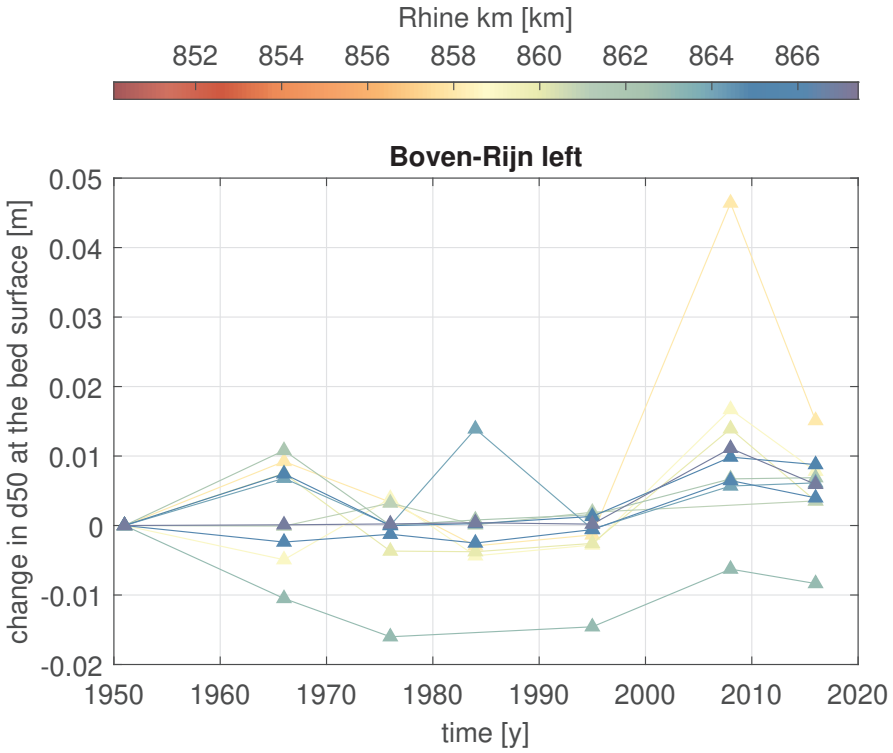

Figure 2.37: *Time evolution of the d_{50} at the bed surface along the left side of the Boven-Rijn relative to the value in 1950.*

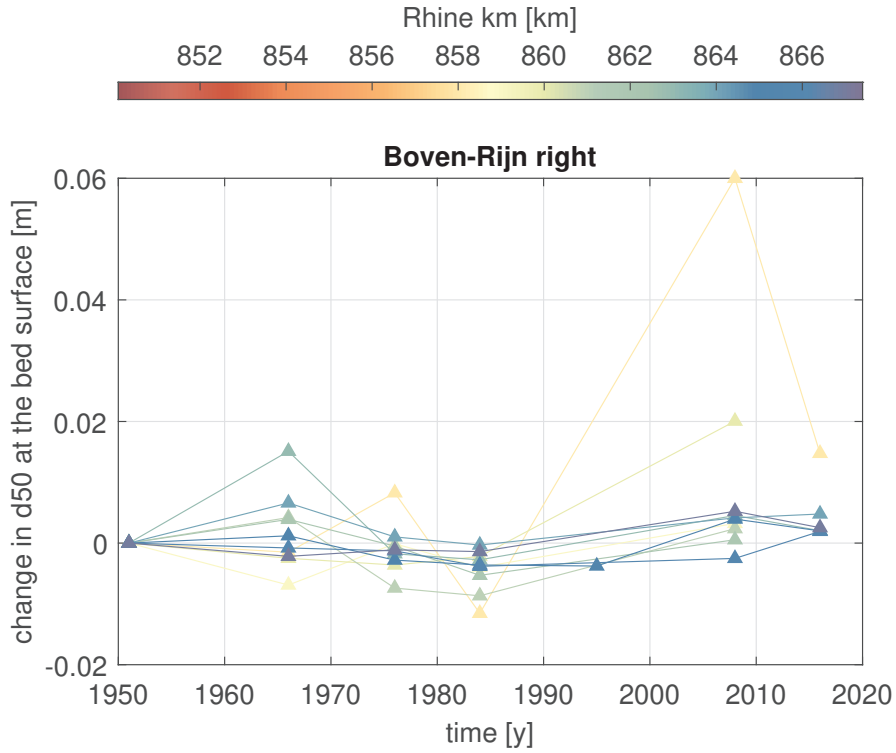

Figure 2.38: *Time evolution of the d_{50} at the bed surface along the right side of the Boven-Rijn relative to the value in 1950.*

3 Modelled development of the Pannerden bifurcation

In this chapter an attempt is made to make a future prediction of bed level development near the bifurcation at Pannerden. To this end, a numerical model is used and compared to past trends. It should be reminded that the model starts in 2015 and ends in 2035, whereas the measured data start well before this period and ends in 2018. In other words, it is difficult to distill whether the model compares well to the measured data, but nonetheless the trends of both model and measurement are analysed.

3.1 DVR Rhine branches model

The DVR Rhine branches model models the Rhine from Xanten (Germany, river-kilometre 824) until the Ketelmeer, the weir at Driel and the Beneden and Boven Merwede. The schematization models mixed-size sediment using 10 characteristic grain sizes. The active-layer thickness is set to a constant value equal to 1 m. The upstream hydrodynamic boundary condition consists of a set of steady discharges ordered to form a characteristic hydrograph. The set of steady discharges is run by means of the Simulation Management Tool (Yossef *et al.*, 2008). The upstream bed level is lowered at a rate equal to 2 cm per year. The sediment transport rate is computed using a calibrated version of the relation by Meyer-Peter and Müller (1948). The simulations model 20 years of morphological development. We refer to Ottevanger *et al.* (2015) for further details on the simulation.

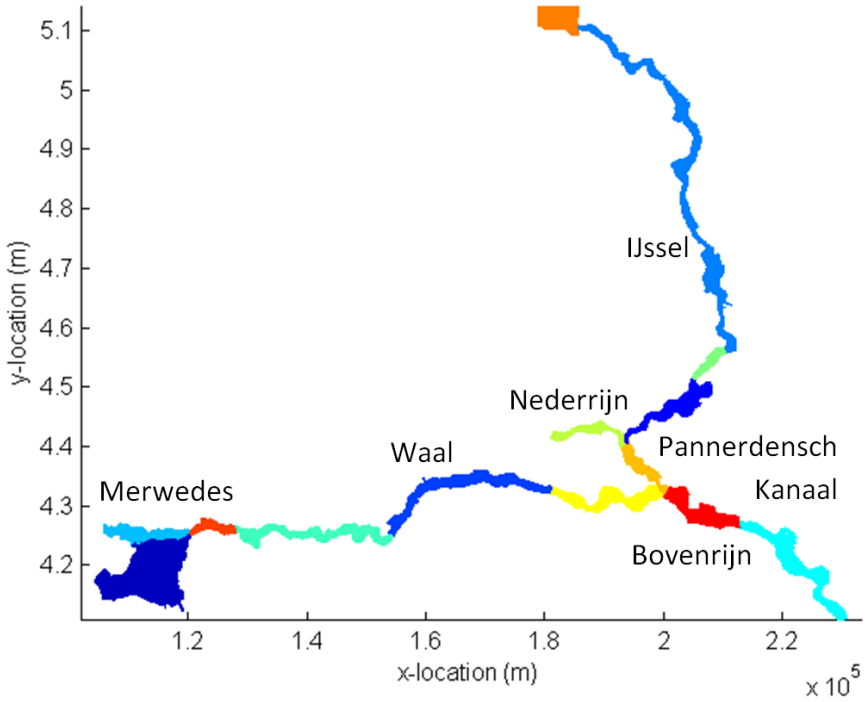

Figure 3.1: *Overview of the domains used in the DVR model*

3.2 Bed elevation

The evolution of the average bed level (averaged over 2 km upstream and downstream of the bifurcation) shows a degrading trend over time. All areas show a degradational trend of roughly –2.5 cm/year. Considering the long-term trend in Figure 2.19, the Boven-Rijn trend is comparable (–2.3 cm/year). A strange jump in the measurements appears just before 2000, which could indicate the long-term trend could be less in the Boven-Rijn. The trend towards the Waal (–1.7 cm/year) and Pannerdensch Kanaal (–4 cm/year) show clear differences. Looking at more recent trends (the past 5 years), it appears the Boven-Rijn and the

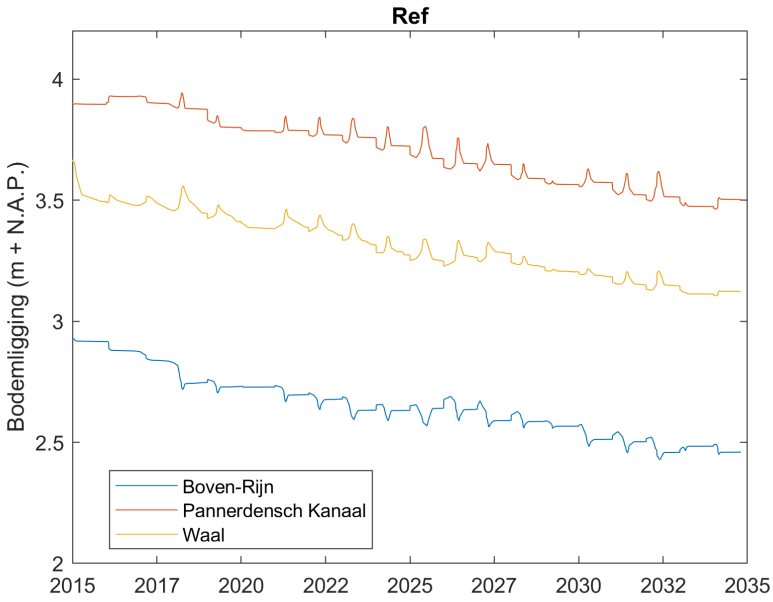

Figure 3.2: *Evolution of the bed level at the Pannerden bifurcation*

Pannerdensch Kanaal have stabilised, whereas the Waal continues to erode at roughly the same rate as the long-term trend. We conclude that the model overestimates the degradational trend around the Pannerden bifurcation.

3.3 Transverse bed slope

The transverse bed level shows a flattening trend just upstream of the bifurcation. This is in contrast to the transverse slope from measurements in Figure 2.11 where it appears to change little in the kilometres just upstream of the bifurcation.

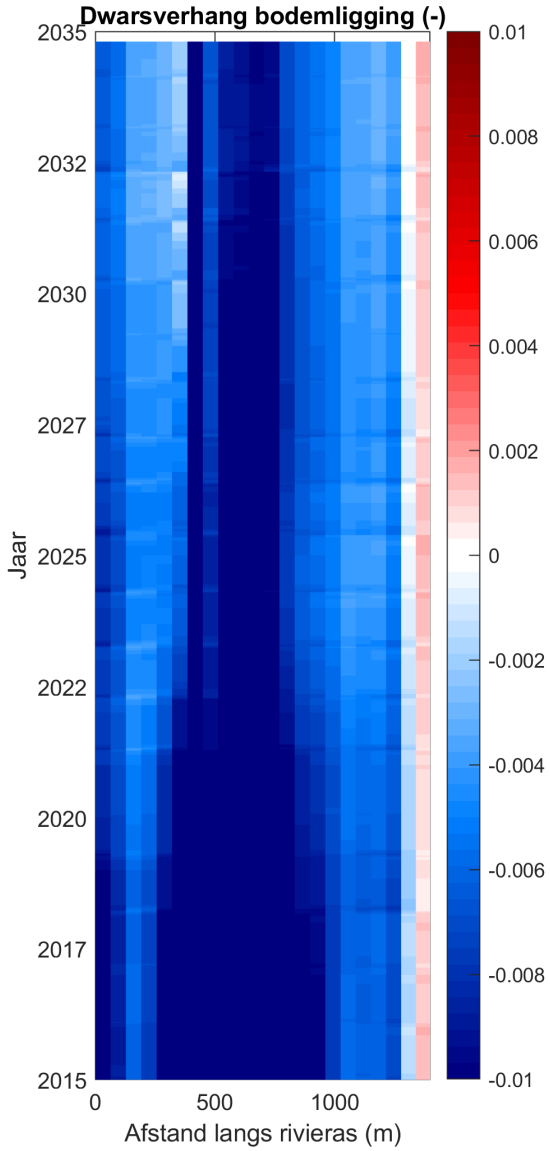

Figure 3.3: *Computed evolution of the transverse slope along the Boven-Rijn just upstream of the the Pannerden bifurcation.*

3.4 Bed level step

The bed level step in the model displays a rather constant pattern. Compared to Figure 2.21 and Figure 2.21 the bed level step from the model is consistently larger. The model also does not capture the reduction of the bed level step towards the Waal which appears from the measurements in recent years. This fits with the observation that the Boven-Rijn bed level is degrading too fast in the model.

Figure 3.4: *Computed evolution of the bed level step at the Pannerden bifurcation*

3.5 Grain size

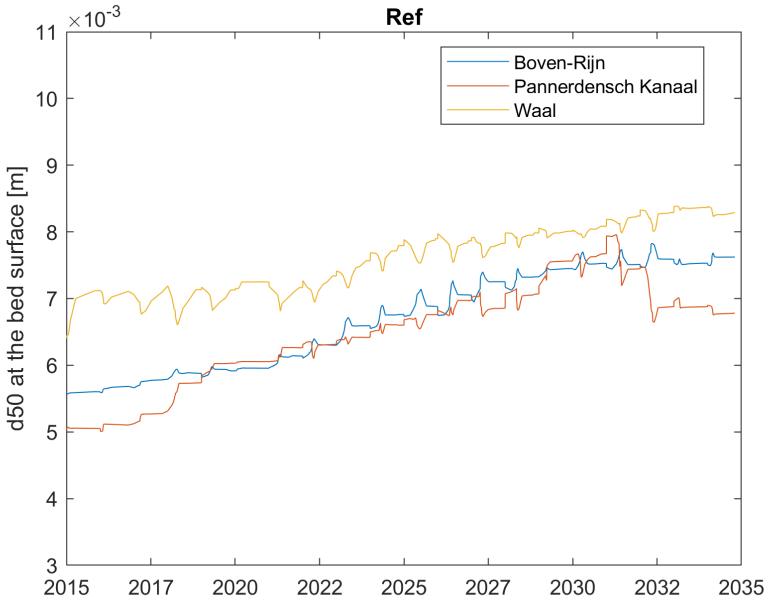

Figure 3.5: *Computed evolution of the mean grain size at the Pannerden bifurcation*

In the model a coarsening trend is found in the region near the Pannerden bifurcation. The mean grain size increases between 1 mm and 2 mm. The comparison to measured grain sizes is not possible as follows from the discussion in Section 2.5.

4 Model sensitivity

In this section we describe the numerical simulations to analyse the sensitivity to bend sorting effects, active-layer properties and hiding and exposure.

The effect of the bed slope on the sediment transport direction is computed using the relation by Koch and Flokstra (1980) in which parameter A_{shld} is a coefficient and parameters B_{shld}, C_{shld}, and D_{shld} are powers of the Shields (1936) stress, the grain size to flow depth ratio, and the grain size to mean grain size ratio, respectively (Deltares, 2013).

Besides the reference run we prescribe six variations to it. The variations are applied to the Boven-Rijn only:

- Case 0: reference (Ottevanger *et al.*, 2015).
- Case 1: No bed level lowering at Xanten
- Case 2: Active-layer thickness equal to 2 m.
- Case 3: Active-layer thickness equal to 0.5 m.
- Case 4: No hiding effect in the Boven-Rijn.
- Case 5: Parameter $C_{shld} = 1.5$ and $D_{shld} = 1.5$.
- Case 6: Parameter $C_{shld} = 0.7$ and $D_{shld} = 0.7$.

We define 4 areas in the bifurcation area in which we average the model results to obtain a representative value. The upstream 2 km is subdivided into left and right sides. Each of the two downstream 2 km are one area each. Figure 4.1 presents the change with time of the bed level step along the Bovern-Rijn - Pannerdensch Kanaal branch. Case 0 and Case 1 present the same results. This indicates that the effect of the upstream boundary condition is not felt in the bifurcation area within 20 years. An active-layer thickness of 2 m keeps the bed level step stable while a thin active-layer thickness equal to 0.5 m causes the bed level step to reduce with time. It stands to reason that the bed level step reacts more slowly to flow changes if the active layer is thicker, as this implies that the grain-size distribution changes more slowly. On the other hand, a thin active layer can lead to fast adaptation of the grain size distribution limiting future changes in bed elevation. Although the active layer affects the transient state but not the equilibrium state in a one-dimensional sense, in a two-dimensional case including a bifurcation and variable discharge, the equilibrium (if any) is expected to depend on the active-layer thickness. Case 3 may be tending to a new equilibrium state.

When not considering the hiding effect (Case 4), the bed level step presents higher variability than when the hiding effect is considered. This is understandable, as hiding causes the sediment transport to behave more closely to how unisize sediment would behave. The effect of the parameters in the closure relation for the effect of the bed slope in the sediment transport direction is crucial. The bed level step is significantly reduced, even reaching a change in sign, when these parameters are modified. Essentially, the bar amplitude and pattern of the bend upstream of the bifurcation are changed, causing overall aggradation.

Considering the more realistic Cases 0, 1, 2, and 3, the bed level keeps constant with time or slightly reduces. On the other hand all simulations predict a decrease of the bed level step between the Boven-Rijn and Waal River (Figure 4.2). Apart from this, the comments on the effect of the variations to the reference case remains equal in this branch.

Cases 5 and 6 cause a physically unrealistic decrease in the transverse bed slope in the bend upstream of the bifurcation, as shown in Figure 4.3. All simulation scenarios except for the one in which we do not consider hiding predict a decrease in the transverse bed slope.

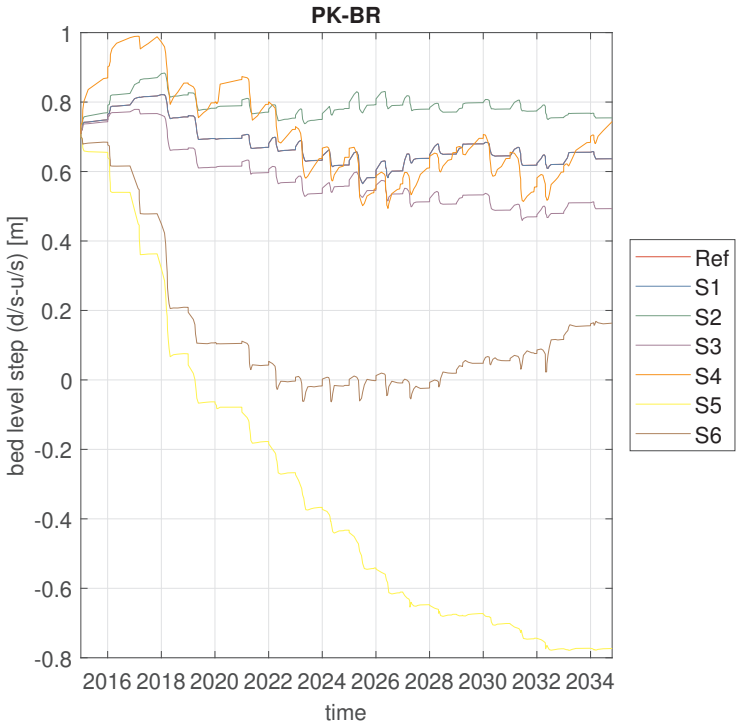

Figure 4.1: *Simulated time evolution of the bed level step along the Boven-Rijn - Pannerdensch Kanaal branch.*

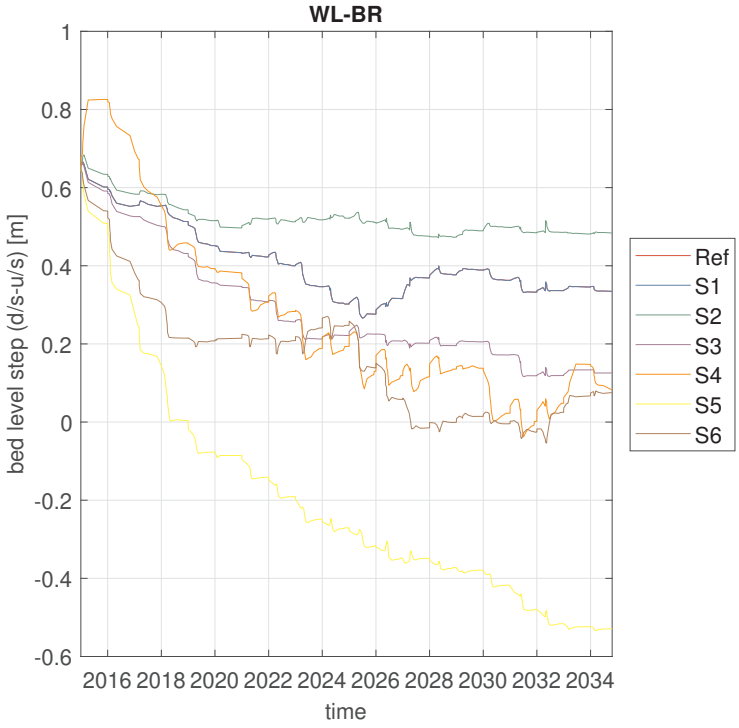

Figure 4.2: *Simulated time evolution of the bed level step along the Boven-Rijn - Waal branch.*

This could mean that the initial bed topography provides a transverse bed slope that is, for all cases, far from the equilibrium transverse bed slope. As in the model results, the measured data show a decrease in the transverse bed slope. However, the measured data predict a smaller change. This indicates that the parameters we use are in all cases not realistic. A calibrated set of parameters would predict flattening of the transverse slope in the upstream bend, but at a slower rate than currently predicted.

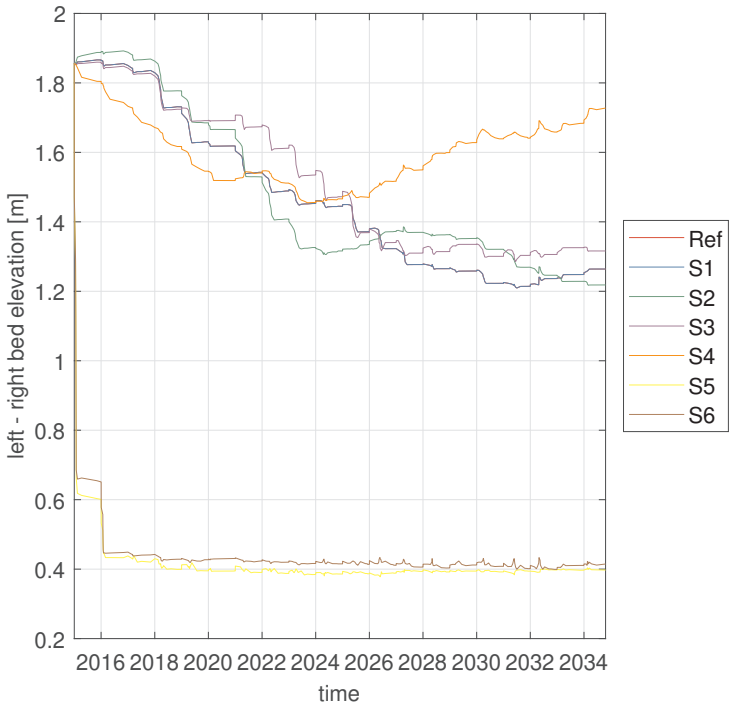

Figure 4.3: *Simulated difference between the bed elevation on the left and on the right hand side along the Boven-Rijn.*

All cases predict a coarsening of the upstream reach (Figures 4.4 and 4.5). The coarsening is substantial, although it cannot be compared to measured data due to the scatter. As with the changes in bed level step, changes are slower when the active layer is thicker. It could be possible that the current situation (i.e., the initial condition) indeed tends to coarsen with time as a reaction to the past river interventions. However, given that the effect of the upstream end is not felt within the domain of interest and the simulation is not long compared to the adaptation time of the Rhine River, the coarsening could be a spurious effect due to using uncalibrated parameters.

The coarsening of the upstream reach causes a coarsening of the downstream reaches for all simulation scenarios except for Case 4 in the Waal River, in which a mild fining is predicted (Figures 4.6 and 4.7). The fact that the upstream reach coarsens does not imply that more coarse sediment is transported downstream. In fact, it seems that the opposite occurs. As hiding is not accounted for, coarse sediment is less mobile and is trapped upstream, causing a fining of the Waal.

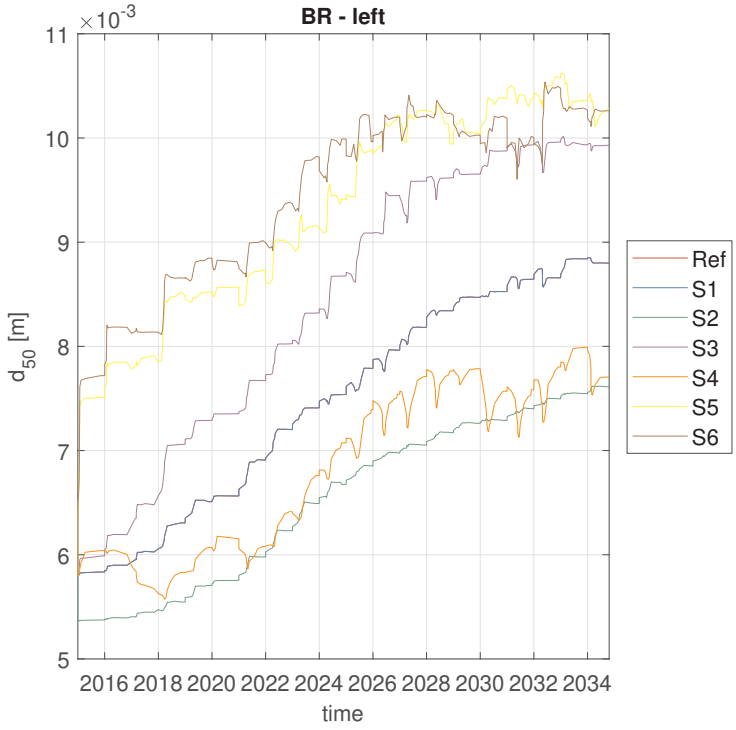

Figure 4.4: *Simulated time evolution of the d_{50} along the left side of the Boven-Rijn.*

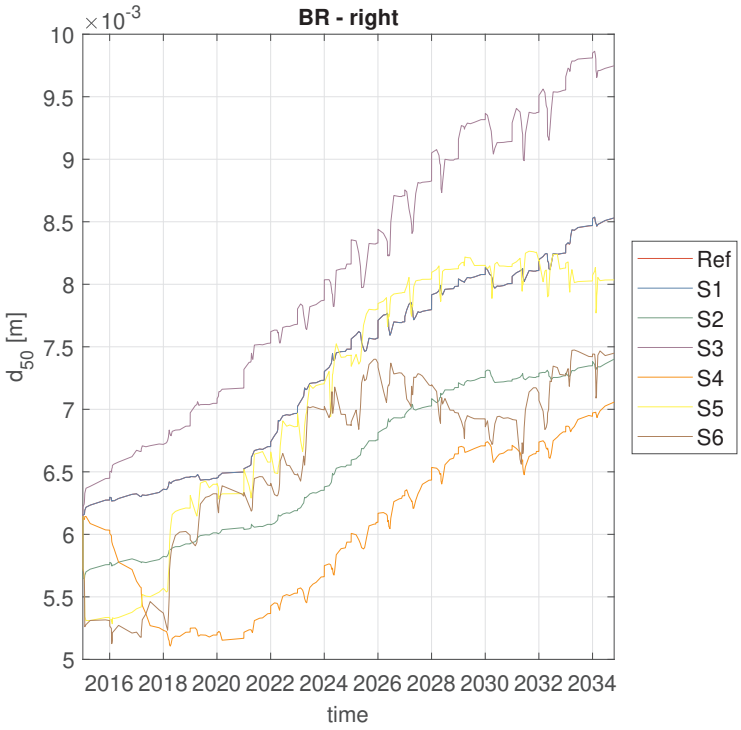

Figure 4.5: *Simulated time evolution of the d_{50} along the right side of the Boven-Rijn.*

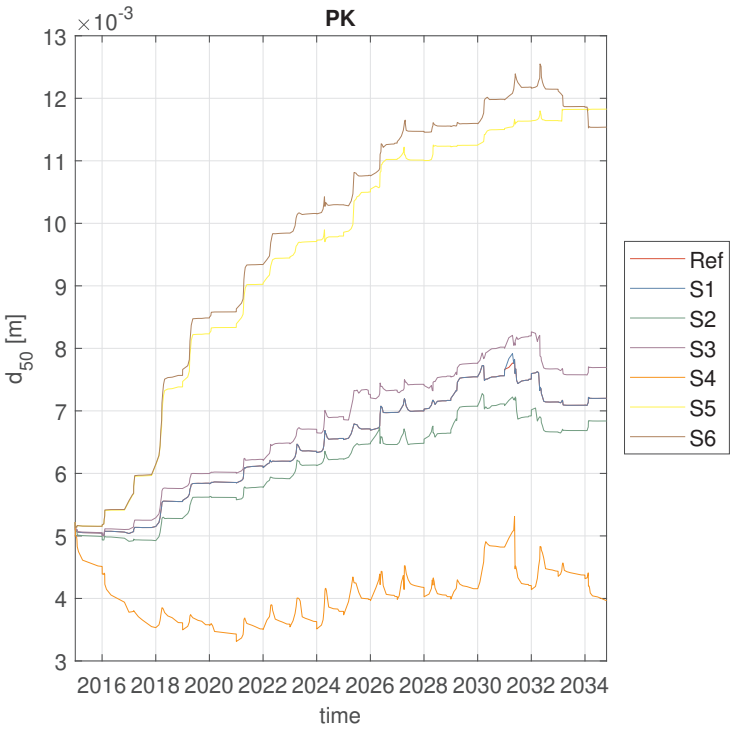

Figure 4.6: *Simulated time evolution of the d_{50} along the Pannerdensch Kanaal.*

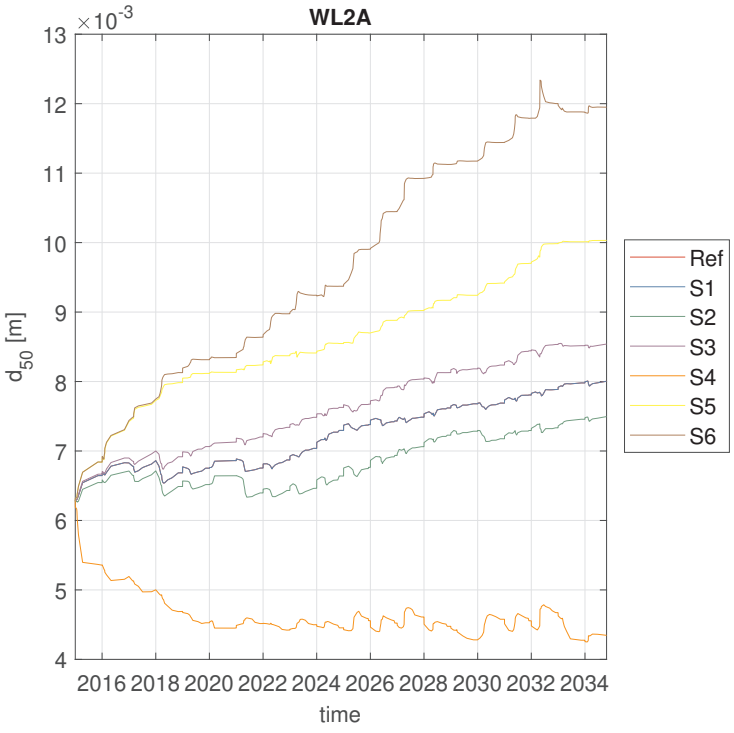

Figure 4.7: *Simulated time evolution of the d_{50} along the Waal.*

5 Predictive function

In this section, we aim at obtaining a function to be able to predict the future state of the bifurcation area based on a reduced set of variables. In particular, we are interested in predicting the future bed level step along the Pannerdensch Kanaal and the Waal. This is because the bed level step is intrinsically related to the water discharge partition, which is the main variable controlling the future of the bifurcation area. Moreover it is expected that the sediment characteristics are linked to the transport and thereby also influence the bed level step. We consider that the bifurcation area is comprised by the last 2 km of the Boven-Rijn and the first 2 km of the Pannerdensch Kanaal and the Waal River. We consider a reduced set of representative variables that account for integrated parameters of the area of interest. Ideally, these variables could be easily measured in the field. The proposed variables are:

- The bed level step along the Pannerdensch Kanaal branch.
- The bed level step along the Waal branch.
- The transverse bed level slope along the Boven-Rijn.
- The characteristic grain size of the left hand side of the Boven-Rijn.
- The characteristic grain size of the right hand side of the Boven-Rijn.
- The characteristic grain size of the Pannerdensch Kanaal.
- The characteristic grain size of the Waal.

A length scale of 2 km implies that the measured data available are limited. For instance, at maximum just four samples of the grain size per branch are available, and for most times even less. Similarly, the measurements of bed elevation prior to the multibeam echosounder provide information averaged over 1 km. Given the scatter in the measured data and the low resolution in measuring both in space and time, we chose to approach obtaining a predictive function based on model results. In the paragraphs we correlate the most important variables of interest based on the numerical results from Chapter 4.

In this section we study the correlation between variables. To this end, we compute the correlation coefficient between the set of variables previously described and the future bed level step in both branches. We consider the future to vary between one month and ten years. An example of the result of this correlation for a 5 years period is given in Figure 5.1. We observe that there is a reasonable amount of correlation between present variables. For instance, the d_{50} of the right hand side of the Boven-Rijn is highly correlated with the d_{50} of the left hand side of the Boven-Rijn. This is not surprising, as it indicates an overall coarsening of the area. There is also a high negative correlation between, for instance, the d_{50} of the Pannerdensch Kanaal and the bed level step along the Pannerdensch Kanaal. This is, again not surprising, as both processes are physically related.

The correlation between the present and the future variables is not significant. Essentially, the present state of the variables cannot be used to predict the state after 5 years.

Certainly, the current state is higly correlated with the future state if it is close enough in time. We study how the correlation coefficients change as the future is further away in time (Figures 5.3 and 5.4 for the bed level step along the Pannerdensch Kanaal and the Waal River, respectively). After only 3 years, the absolute correlation coefficient for all variables is lower than 0.6, which indicates that variables are poorly correlated. For completeness, and to show that the approach of using the correlation is justified, no clear function can be found particularly comparing the current to the future data. This is shown in Figure 5.2.

We conclude that a simplified analysis by seeking correlations between integrated parameters

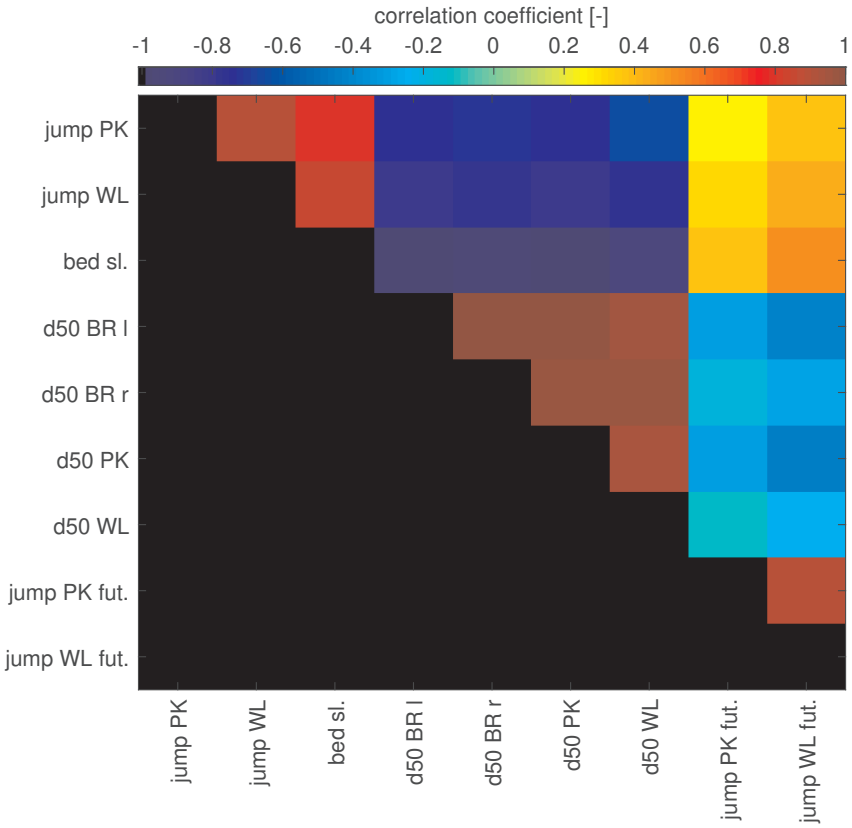

Figure 5.1: *Correlation coefficients between variables for a 5 years prediction. The labels from top to down and left to right indicate the bed level step along the Pannerdensch Kanaal, the bed level step along the Waal, the transverse bed slope of the Boven-Rijn, the d_{50} of the left hand side of the Boven-Rijn, the d_{50} of the right hand side of the Boven-Rijn, the d_{50} of the Pannerdensch Kanaal, the d_{50} of the Waal, the future bed level step along the Pannerdensch Kanaal, and the future bed level step along the Waal.*

is not successful. Moreover, it is questionable if such a relation could be used, as the grain size measurements seem quite uncertain.

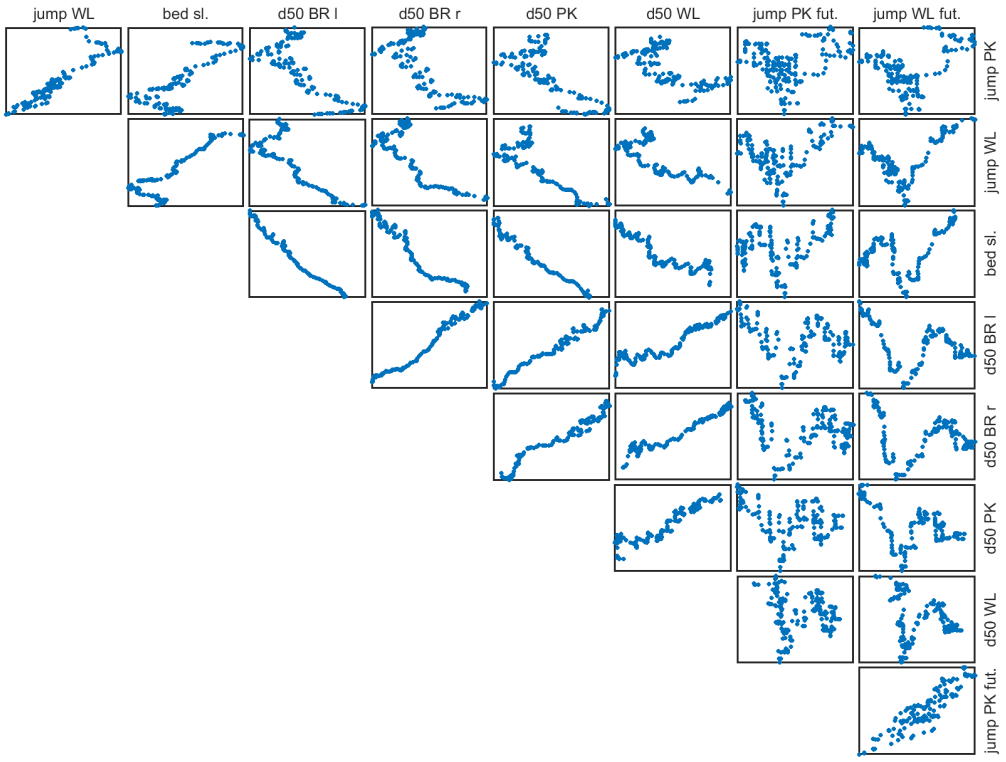

Figure 5.2: *Underlying data used for determining the correlation coefficients.*

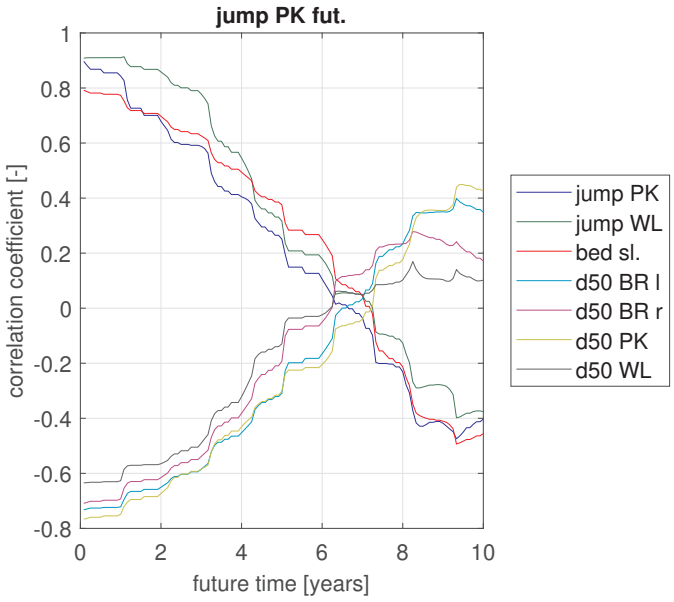

Figure 5.3: *Correlation coefficients for predicting the bed level step in the Boven-Rijn - Pannerdensch Kanaal branch as a function of the prediction span.*

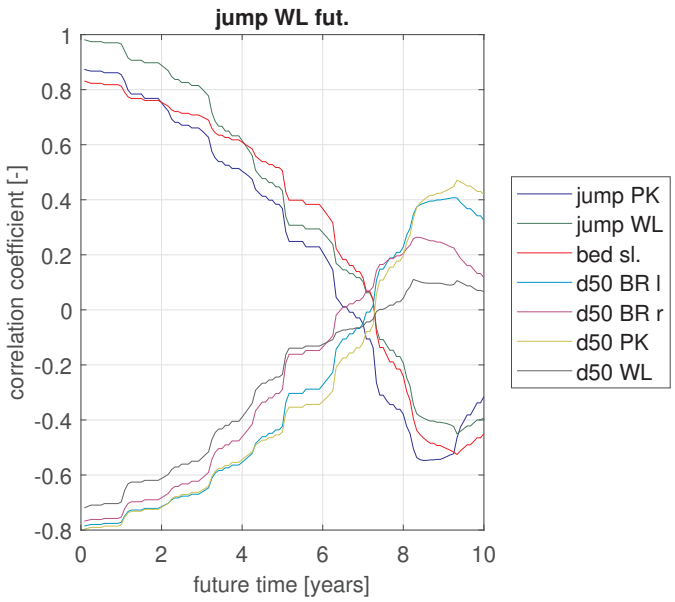

Figure 5.4: *Correlation coefficients for predicting the bed level step in the Boven-Rijn - Waal branch as a function of the prediction span.*

6 Modelling of armoured layers

The concept of semi-fixed layers was introduced by Tuijnder and Ribberink (2010a) which was subsequently implemented in a research version of Delft3D 4 (Tuijnder *et al.*, 2011). This was applied to the Pannerden bifurcation (Tuijnder *et al.*, 2012), showing promising results. Within an earlier KPP Rivierkunde project this version was ported to the DAD_uniform_graded branch (Ottevanger, 2015) `https://svn.oss.deltares.nl/repos/delft3d/branches/research/Deltares/20130603-DAD_uniform_graded` revision 5220.

Although a simple test case showed that the model behaviour was similar to the software in (Tuijnder *et al.*, 2011) `https://svn.oss.deltares.nl/repos/delft3d/branches/research/Deltares/20121113-Semi_fixed_layers` revision 2186, the simulation for the full Rhine model showed strange results. Moreover the results of the simple testcases also showed strange results which required further explanation.

The changes have been ported to the current Delft3D-4-DVR executable `https://svn.oss.deltares.nl/repos/delft3d/branches/research/Deltares/20170214-Delft3D-4-DVR` revision 65334 and compilation has been made possible for the Intel 14 compiler in combination with Microsoft Visual Studio 2012. This is important as the DVR simulation requires certain features that are not available in the main version of Delft3D. By this merging of code lines the Delft3D-4-DVR code now includes the code by (Tuijnder *et al.*, 2011).

In this chapter the simple testcases are repeated for the new code. Subsequently the results are analysed, and based on these findings a real-world application using this functionality is performed.

6.1 Simple testcases inspired by Struiksma (1999)

For the testing of the code by Tuijnder *et al.* (2011) a test case was developed resembling the experiment by Struiksma (1999). Rather than including a fixed layer, however, a second coarse immobile sediment fraction was included. The initial sediment volume fraction is shown in Figure 6.1. The initial slope in the bed level in the simulation is based on the equilbrium slope based on the fine sediment fraction. The discharge is set to 9.2 l/s and the downstream water level is set to 0.34 m and the width of the flume is 0.2 m.

Multiple sensitivity runs were performed using this code similar to Ottevanger *et al.* (2015) to understand the influence of certain input parameters related to this code. These cases are repeated in this research and the behaviour is further analysed, to explain the strange results reported previously and to verify that the implementation of the code is the same. An overview of the simulations and the most important parameters is given in Table 6.1. For all simulations the alluvial active-layer thickness is described as proportional to the dune height by the factor *TTLAlpha*. In all cases the dune height is assumed to be one fifth of the water depth. The other parameters of the simulation are discussed when introducing the modelling concepts in Section 6.2.

The results of the simple testcases are found to produce the same results as before, thereby showing that the functionality is the same as in the original implementation (see Appendix A, cf. Ottevanger (2015)).

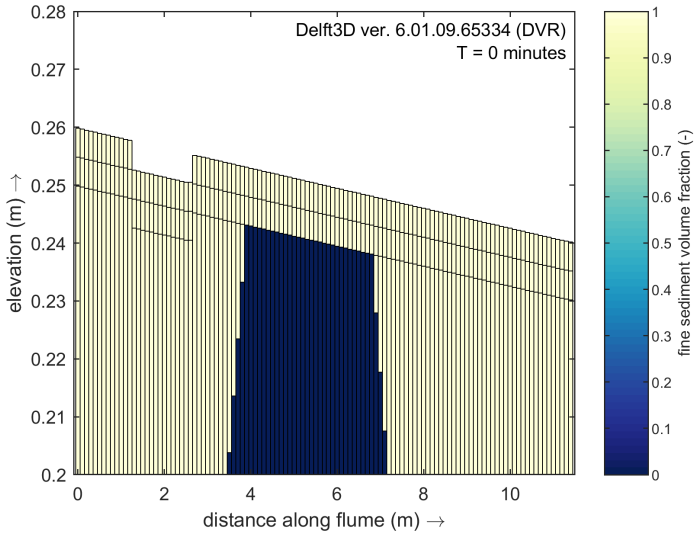

Figure 6.1: *Initial sediment volume fraction in the bed for case C1*

Table 6.1: *Overview of simulations for the transport of coarse immobile sediment*

Simulation	IMobility	Description	Amax [-]	SincFracMax [-]	ThCLyr [m]	ThTrLyrTa [s]	TTLAlpha [-]
C0	-	No coarse layer	-	-	-	-	1.5
C1	0	Discrete model	20	0.01	0.005	180	1.5
C2	1	Shields (1936)	20	0.01	0.005	180	1.5
C3	2	Wilcock and McArdell (1997)	20	0.01	0.005	180	1.5
C4	2	Characteristic length scale of dune troughs	40	0.02	0.005	180	1.5
C5	2	Coarse layer thickness	20	0.01	0.01	180	1.5
C6	2	Adaptation time of the transport layer	20	0.01	0.005	360	1.5
C7	2	Equilibrium dune height	20	0.01	0.005	180	0.75
C8	-	Fixed layer	-	-	-	-	1.5
D0	-	No coarse layer	-	-	-	-	0.25
D1	0	Discrete model	20	0.01	0.005	180	0.25
D2	-	Fixed layer	-	-	-	-	0.25

6.2 Analysis of modelled transport over coarse immobile layers

To research the behaviour of the Tuijnder *et al.* (2011) concept two cases are highlighted. These are the C0 and C1 cases. The C0 case uses the standard Hirano (1971) model without any adjustment and the C1 case is based on the Tuijnder *et al.* (2011) concept.

The Hirano (1971) model consists of an active layer with multiple sediment fractions. For each sediment fraction in the active layer, transports are computed and their relative contribution within the active layer may also be used in the hiding-and-exposure correction for sediment entrainment. After computation of the transports per fraction, the sum of the outgoing and incoming sediment in a control volume will equal the overall change in the bed level. When using the Hirano model the active layer will continue to have the same thickness, and if there is overall erosion, sediment will be replenished from the sediment just underneath the active layer. When there is overall sedimentation, sediment will be moved below the active layer. The active-layer thickness in the case of enough sediment is referred to as the alluvial active-layer thickness. When sediment is not available beneath the active layer to replenish it to its alluvial thickness, e.g. in the case of a fixed layer, the active layer reduces to the available thickness of sediment. In the case the active-layer thickness reduces below the alluvial active-layer thickness (in the case of too little sediment) the sediment transport is reduced by the ratio of the actual to the alluvial active-layer thickness according to the theory of Struiksma (1999)

extended to multiple fractions.

The concept developed by Tuijnder *et al.* (2011) introduces a coarse layer in to the Hirano (1971) model just below the active layer, which maintains a certain prescribed thickness (*ThCLyr*), where the sediment is available. If there is insufficient material to fill the coarse layer and the alluvial active-layer thickness, the material can reside in the active and the coarse layer. Where it resides depends on different processes. Sediment in transport is only present in the active layer, and sediment which is not mobile is moved from the active to the coarse layer. This happens by way of different mobility functions defined using the *IMobility* keyword and related to parameters governing the sorting speed *Amax* and *SinkFracMax*. By way of immobility of certain sediment fractions the active-layer thickness can reduce, thereby again limiting the transport such as the case of the Hirano model over a fixed layer using the concept of Struiksma. When the sediment in the coarse layer becomes mobile again, the active-layer thickness grows thereby taking sediment from the coarse layer, which in turn is replenished by sediment from underneath the coarse layer to maintain the prescribed thickness. Besides that there is an adaptation timescale included, *ThTrLyr* ensures that a certain time is required before the active layer reaches the alluvial thickness. Further details can be found in Tuijnder *et al.* (2011).

Figure 6.2 and Figure 6.3 show the sediment content in the bed after one day, for the case using the Hirano concept (C0) and the case using the Tuijnder concept (C1), respectively. The discussion will be limited to these two cases and the C8 case consisting of a single fraction and a fixed layer, as the other simulations (C2-C7, shown in Appendix A) show behaviour which can be explained by a combination of the limits of C0 and C1.

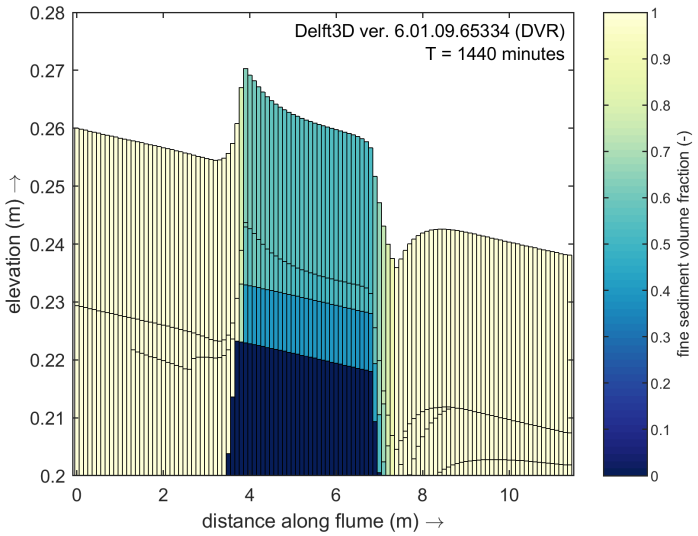

Figure 6.2: *Final sediment volume fraction in the bed for case C0*

For the Hirano case C0, as the trench moves over the patch of coarse sediment it becomes apparent that coarse immobile material enters into the active layer thereby forming a mixture. The formation of a mixture has two effects on the transport, namely: the transport of the fine fraction is reduced due to the presence of other not mobile material, and due to hiding-and-exposure effects the transport of the fine fraction may be limited even further. These effects combined result in sedimentation over the coarse patch which essentially becomes shallower to match the equilibrium transport at the upstream boundary.

For the Tuijnder case C1, as the trench passes over the coarse immobile patch, the resulting

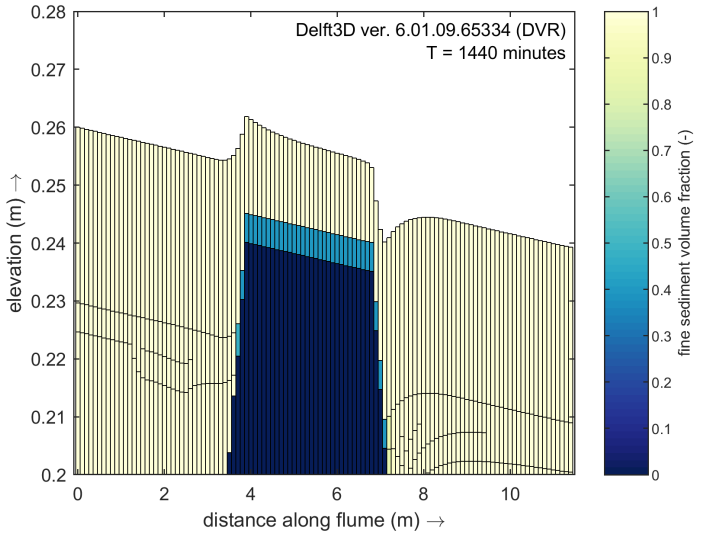

Figure 6.3: *Final sediment volume fraction in the bed for case C1*

bed level is similar. However, the sediment fraction content is different. In this case the transports over the coarse immobile patch are reduced during the passage of the trench by the reduction of active-layer thickness due to the presence of a coarser layer by the Struiksma concept. Similarly sedimentation occurs until the net transport (= reduction factor $\times$ alluvial sediment transport) is in equilibrium again.

This increase in bed level over the coarse patch looks unphysical and in both cases the apparent cause is the definition of the active-layer thickness. One would hope to see a return to the equilibrium slope as in the case of the Struiksma (1999) experiment. However, by way of the imposed alluvial active-layer thickness the transport over the active layer is reduced. This however would also be the case when modelling a single fine fraction over a fixed layer as well when using the same active-layer thickness. This was verified using the C8 case (cf. Figure 6.4)

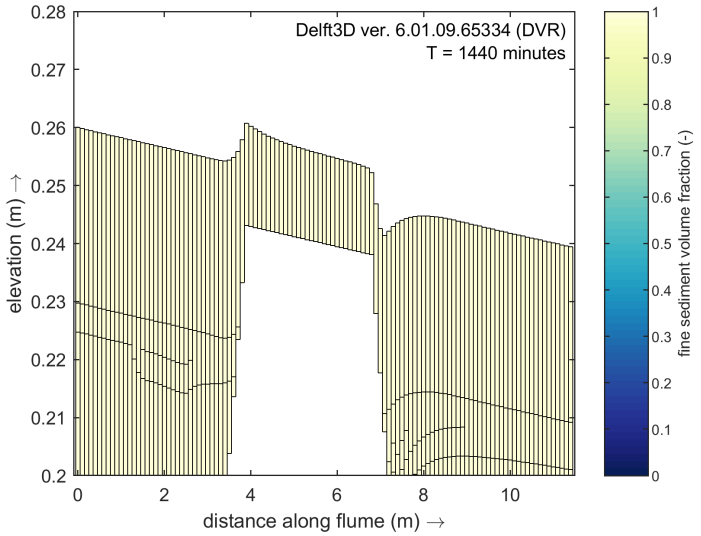

Figure 6.4: *Final sediment volume fraction in the bed for case C8*

Including an alluvial layer thickness which is much smaller than the layer thickness above the coarse sediment shows similar behaviour for the bed level for D0, D1, and D2 (cf. Figures 6.5 - 6.7). The Tuijnder approach shows some fining of the coarse layer which is kept at a fixed thickness.

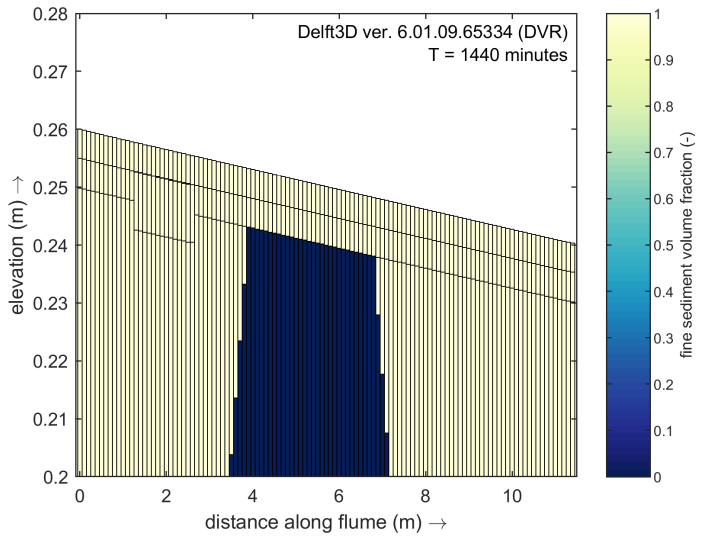

Figure 6.5: *Final sediment volume fraction in the bed for case D0*

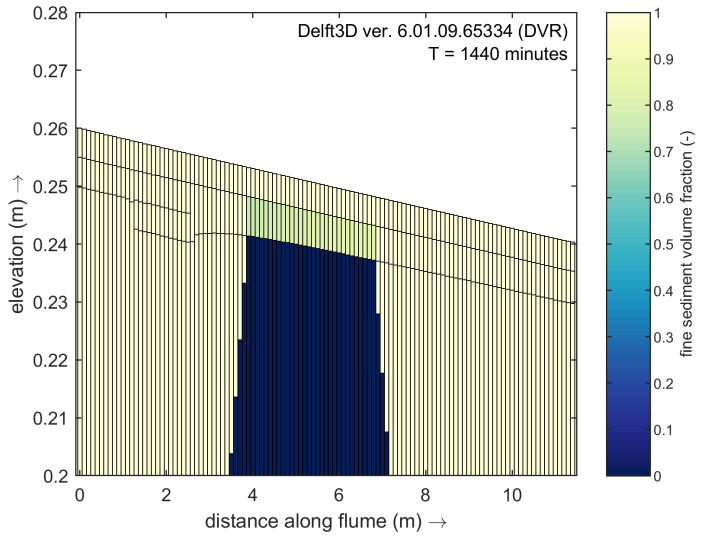

Figure 6.6: *Final sediment volume fraction in the bed for case D1*

From this investigation, we can conclude that the behaviour of the models is very sensitive to the thickness of the active layer and the computed sediment transport, which may also be reduced to the active-layer thickness in the case Struiksma is activated. The importance of the active-layer thickness has long been known. However, this investigation shows that it is very important to have a correct active-layer thickness and a correct prediction of sediment transport in the case that the supply of sediment is limited. It is likely that this needs further investigation when modelling the sediment transport over armoured layers, and it is unclear whether the existing modelling concepts offer enough to model this accurately. It should be added that current experimental evidence is probably also not sufficient to prove which theory accurately describes this behaviour.

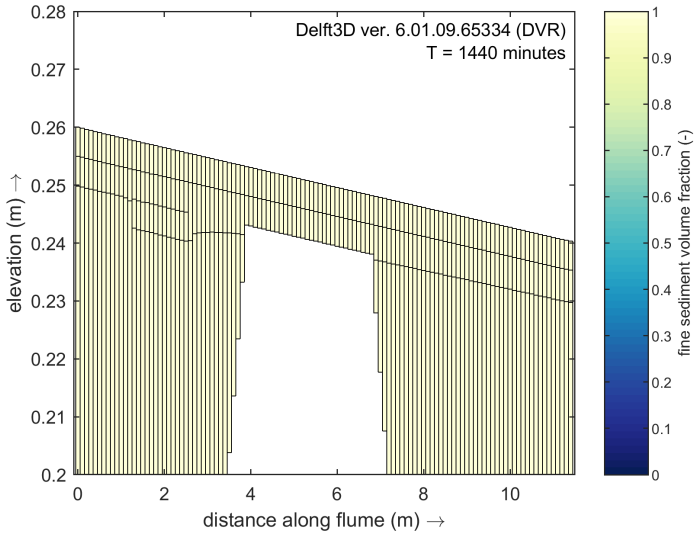

Figure 6.7: *Final sediment volume fraction in the bed for case D2*

6.3 Application of modelling concepts to Rhine branches simulation

Based on the previous Section 6.2, two simulations are performed with the DVR model and a constant alluvial active-layer thickness of 1 m. The first T1 is based on the standard Hirano approach, whereas the second uses the Tuijnder approach using settings similar to Tuijnder *et al.* (2012). These are summarised in Table 6.2.

Unfortunately, the T2 simulation crashed after 2 years of simulation time, due to some instability which was not further analysed.

Therefore we looked at the outcome of the simulation after 2 years. The results in Figure 6.8 and Figure 6.9 indicate that the T2 simulation is unstable, and needs further investigation to find out what is going wrong.

Figure 6.8: *Bed level changes after two years for case T1*

Table 6.2: *Overview of simulations for the transport of coarse immobile sediment applied to the DVR model*

Simulation	IMobility	Description	Amax [-]	SincFracMax [-]	ThCLyr [m]	ThTrLyrTa [s]	ThTrLyr [m]
T1	-	Hirano (1971) No coarse layer	-	-	-	-	1.5
T2	2	Tuijnder *et al.* (2011) using Wilcock and McArdell (1997)	20	0.05	0.05	18000	1.0

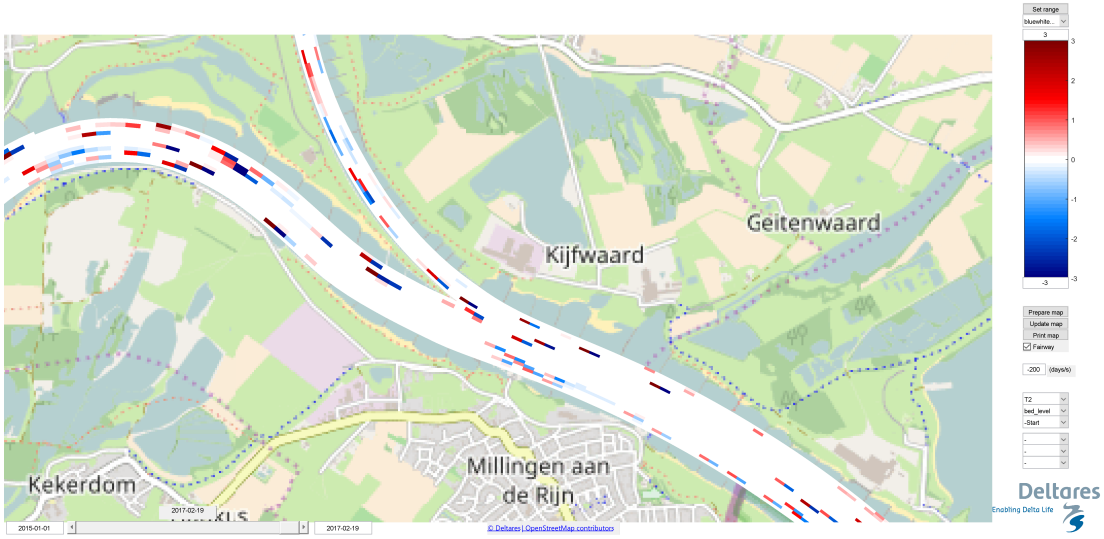

Figure 6.9: *Bed level changes after two years for case T2*

6.4 Discussion on the modelling of armoured layers

Rijkswaterstaat, as manager of the Dutch river system, is interested in predicting morphodynamic changes. Several tools are used for this purpose and one of the tools is numerical models. In all current numerical models (e.g., Delft3D-4 and Delft3D-FM), the predicted bed elevation and grain size distribution represent values averaged over the passage of several bedforms. Worded differently, the effect of individual bedforms is not modelled. Changes in bed elevation are predicted on the basis of gradients in the total sediment transport rate (i.e., we solve the Exner (1920) equation). Changes in grain size distribution of the bed surface are predicted on the basis of gradients in the sediment transport rate of each size fraction and fluxes between the bed surface (i.e., the active layer) and the substrate (i.e., we solve the Hirano (1971) active-layer equation). Sediment in the active layer plays a role in the sediment transport rate. The sediment in the substrate is assumed to be too deep to play a role in the sediment transport rate. The system of equations requires a closure relation that predicts the sediment transport rate per size fraction based on the composition of the bed surface. This closure relation needs to account for the fact that fine grains in a mixture of sediment of different sizes hide behind coarse grains and are thus less exposed to the flow than under unisize conditions (Einstein, 1950).

The active-layer model is dependent on a crucial parameter: the active-layer thickness. This parameter sets the part of the bed that interacts with the flow. This is essentially different from the bed load layer thickness (e.g., Van Rijn (1984); Luu *et al.* (2004); Wu and Yang (2004); Colombini (2004); Colombini and Stocchino (2005)) which represents the part of the bed that is moving. The sediment in the active layer is available for being transported and sediment in transport deposits in the active layer. For this reason, the thickness of the bed load layer in a

fully immobile bed is equal to 0, but not the active-layer thickness. Under plane-bed conditions and on short time scales, the active-layer thickness is usually associated to a characteristic grain size of the bed surface, and under bedform-dominated conditions the part of the bed that interacts with the flow is usually related to a characteristic bedform height. In general, the active-layer thickness covers a significant percentage (e.g., 95%) of the probability distribution of bed elevation fluctuations around the mean value (averaging over the passage of several bedforms) (Ribberink, 1987; Blom *et al.*, 2003).

In a situation in which there are no gradients in the sediment transport rate per size fraction (and as such the mean bed elevation is constant), the only process that can lead to a change in surface grain size distribution is a lowering of the interface between the active layer and the substrate due to, for instance, an increase in the active-layer thickness. This is a limitation of the active-layer model, as several processes are inadequately described in this manner. For instance, dune growth under normal flow conditions (i.e., without change in mean bed elevation) causes the formation of a coarse layer underneath migrating dunes (Blom *et al.*, 2003). Lee-face sorting causes the deposition of coarse sediment at the dune troughs. As it often happens, the coarse sediment is immobile and dunes become composed of the fine fractions only. The coarse layer inhibits the entrainment of fine sediment and limits the sediment transport rate. Although the formation of such a coarse layer is not modelled by the active-layer model, the active-layer model does account for the transport of some of the sediment fractions while some other sediment fractions remain immobile. Whether a particular sediment fraction is mobile or not depends on the closure relation for the sediment transport rate (considering hiding) and the amount of the particular sediment fraction relative to the total sediment at the bed surface (i.e., in the active layer). The reduction in sediment transport is intrinsic to the fact that there is sediment in the active layer which is not mobile.

A similar situation to the one in which dunes composed of fine sediment travel on top of a layer of coarse immobile sediment is that of unisize sediment transported on top of a fixed layer. Predicting morphodynamic changes under these conditions is of importance for Rijkswaterstaat, given the constructed fixed layers (e.g., at Nijmegen) as well as the naturally present ones (e.g., clay patches). Struiksma (1999) developed a model for predicting unisize morphodynamic changes under these conditions. He observed that the sediment transport rate on top of a fixed layer is reduced compared to a case in which no fixed layer is present (as it happens in the lee-face-induced case). In accounting for this process, Struiksma (1999) introduced the concepts of the “thickness of alluvium” and the “maximum thickness of alluvium at which the non-erodible layer affects the sediment transport”. The thickness of alluvium represents the thickness (averaged over several bedforms) of sediment above a non-erodible layer.

In extending the concept of Struiksma (1999) to mixed-size sediment conditions, there are two straightforward possibilities. The active layer (in the mixed-size sediment model) can be considered to be equivalent to the thickness of alluvium or to the maximum thickness of alluvium (in the unisize model).

In the first case (i.e., the active-layer thickness is equivalent to the thickness of alluvium), by definition, immobile sediment does not form part of the active layer. The active layer is composed of mobile sediment only. This poses conceptual incongruences for the reasons that follow. Considering the time scale used in averaging the bed elevation (i.e., the passage of several bedforms), immobile sediment in a fixed layer high enough to affect the sediment transport rate is at some moments exposed to the flow. This means that immobile sediment influences the flow (e.g., affecting friction) and is available for being transported. Thus, according to the definition of the active layer, immobile sediment should form part of the active layer. Note also that immobile sediment would immediately become mobile if the flow conditions suddenly change, without the need of bedform dimensions to adapt to the new flow

conditions. That is, immobile sediment may become mobile without a change in active-layer thickness (i.e., without entraining substrate sediment). This process is not possible to model if immobile sediment is not present in the active layer. Essentially, if a fixed layer is sufficiently close to the mean bed elevation such that it affects the sediment transport rate, the elevation of the fixed layer is within 95% of the bed elevation fluctuations around the mean value, which implies that the fixed layer must form part of the active layer.

The above reasons suggest that the active layer must be taken equivalent to the maximum thickness of alluvium. Then, immobile sediment in a fixed layer is transferred to the active layer when the fixed layer is high enough. In this case, the reduction of the sediment transport rate that the unisize model predicts (Struiksma, 1999) is implicitly considered in the mixed-size sediment model, as we have previously explained.

The *Plan van Aanpak* of this project proposed adapting the model developed by Tuijnder and Ribberink (2010b, 2012) for "semi-fixed layers" in order to account for morphodynamic development under mixed-size sediment conditions in the presence of fixed layers. This model differs from the active-layer model in that it accounts for the lee-face mechanism that causes the formation of a coarse layer. A layer is introduced between the active layer and the substrate that, even under normal flow conditions (i.e., without changes in mean bed elevation), coarsens when only fine sediment is transported. For this reason, this model not only aims at modelling sediment transport over a coarse layer (which, as we have seen, the active-layer model does) but also aims at modelling the vertical sorting that occurs under these conditions (given that the bed is bedform dominated).

Tuijnder and Ribberink (2012) are right in pointing out that the model developed by Struiksma (1999) is not capable of modelling the break-up of an armour layer. In the unisize model by Struiksma (1999) the armour layer is fixed. This justifies the development of a new model. However, the active-layer model can account for the break-up of an armour layer. Essentially, when the bed shear stress is sufficiently high to mobilize the coarse sediment size fractions, the sediment transport rate will suddenly increase and coarsen, indicating the break-up of the armour. The characteristic that the active-layer model cannot reproduce (and thus justifies the development of a new model) is the temporal evolution during the break-up (and formation) of an armour layer.

In modelling the transport of fine sediment over a coarse layer, there is no need to develop a new model, as the active-layer model accounts for this process. The model by Tuijnder and Ribberink (2010b, 2012) is of interest if we aim at modelling the formation of the coarse layer. Although this is a topic for further discussion, we advance that, at this moment, we do not recommend applying the model by Tuijnder and Ribberink (2010b, 2012) for such end. This is because we find a conceptual problem. While the sediment in the active layer of the active-layer model is the sediment that interacts with the flow (mobile or immobile), the sediment in the active layer of the model by Tuijnder and Ribberink (2010b, 2012) is only the mobile sediment. However, the sediment that is in transport (i.e., the one computed by means of the sediment transport closure relation based on the properties of the active layer) is also defined as the sediment that is mobile. Moreover, as the sediment in transport depends on the (mobile) sediment in the active layer, the coarse sediment exposed to the flow has no influence on computing the sediment transport rate.

Two more issues related to the model by Tuijnder and Ribberink (2010b, 2012) are that: (1) previous field scale results cannot be reproduced (Ottevanger, 2015, and the current study) and (2) the model incorrectly predicts the dynamics at the model boundaries (Tuijnder *et al.*, 2012). Both of these issues may be related to either implementation of the modelling concept or to unstudied conceptual problems, or both.

7 Conclusions

We have studied the change with time of the bed elevation, transverse bed slope, bed level step and sediment grain size in the area around the bifurcation at Pannerden using measured data. Certain measurements show some yet unexplained artefacts (e.g. bed level step in Boven-Rijn just before 2000). The change in measuring technique may explain the disagreement, but it is not yet conclusive. Nevertheless, the data show a clear overall degradational trend. The transverse slope of the downstream part of the Niederrhein has decreased with time. Dredging activities and surface coarsening explain this trend, but other factors may play a role.

Rijkswaterstaat is interested in answering questions regarding changes in grain size distribution. For instance, it would be of interest to be able to predict the future development around the bifurcation area based on the current state of bed armouring. We have shown that the available data are insufficient to answer questions regarding changes in grain size distribution. For this reason, it is currently not possible to assess future trends such as the effects of climate change based on the available data.

We have studied the trends using predictions based on Delft3D-4-DVR simulations. The measured and modelled trends in bed elevation and the model results show differences. An important factor explaining the differences is that the model covers a different period of time than the measured data and the fact that the model has not been calibrated. The overall modelled degradation around the bifurcation area compared to the measured data in recent years suggests that the transport in the model may be too low in the Boven-Rijn and too high in the downstream branches, and that the sediment data included in the model need updating. Besides that, the role of dredging maintenance as included in the model may need further refinement. The study on model sensitivity shows the effect of varying multiple parameters related to morphodynamic development and indicates that there is a need to invest in a detailed calibration of the model.

A simplified predictive function appears to be not readily possible, neither based on the model results, nor based on the currently available measurements. The impossibility of finding simple relations emphasizes the need of a calibrated model.

As requested by Rijkswaterstaat, we have studied using the implementation of the modelling concept developed by Tuijnder and Ribberink (2012) in Delft3D for improving the modelling predictions. Their modelling concept was in a research branch and had to be merged within the new code to be able to run it. We have managed to run new simulations using the modelling concept developed by Tuijnder and Ribberink (2012). Test simulations at small laboratory scale show reasonable results. A large-scale application shows physically unrealistic patterns of aggradation and degradation. We have conducted a first analysis on how to model the formation and break-up of armour layers (Section 6.4). We conclude that there is a need to study the possibility of adapting the active-layer model to this end.

Regarding the still open research question for this report whether coarse nourishments can be used to stabilize the bed level in the degrading parts of the Rhine, the answer is that it should be possible, as shown by Ottevanger *et al.* (2015). In this research, a yearly recurring nourishment was performed stabilizing the bed in the Boven-Rijn and Pannerdensch Kanaal. The drawback, however, was that in doing so the discharge distribution tended to increase more to the Waal and it is unclear whether this extra flow towards the Waal is only beneficial, or that extra erosion may also need to be counteracted here by nourishments as well. Another matter of concern is whether or not the nourished material can be found and at what cost this

is available. In the study for the Boven-Rijn nourishment the thickness of the nourishment considering a total volume was varied (Niesten *et al.*, 2017), but the effect of the coarseness of the material to be nourished was not varied. The expectation is, however, that coarser sediment will remain in place longer compared to a finer nourishment, but will cause a temporary degradational wave downstream of the nourishment. The exact response is hard to predict exactly as found from the simulations performed in Chapter 6.

8 Recommendations

8.1 Long-term prediction

For the long-term prediction of the Rhine branches, we recommend performing a further calibration of the model. A possible starting point could be the ongoing research of the longitudinal training walls in the Waal (Omer, 2019) or the ten-year hindcast performed in KPP river engineering (Ottevanger, 2017). In addition, it is recommended to generate a schematic idealised case resembling the Rhine branches, and gradually increase the complexity towards the full-complexity model.

From a nonlinear phase-plane-stability analysis (Wang *et al.*, 1995), we know that bifurcations may be quasi-stable (slowly evolving) for a long time and then suddenly lose stability. Delft3D might be used to mimic this in order to timely identify critical states that are close to the transition from quasi-stable to unstable (cf., Scheffer *et al.* (2012)).

It is noted that the grain size data are very uncertain in Rhine branches. For the future, it is recommended to gain insight into the sediment properties both at the bed surface and below the bed surface, such that we are able to better understand the morphological behaviour of the river. Furthermore, it is recommended to formulate a strategy for measurement of the grain size distribution, or reanalysis of previous raw data, such that these data can be used in the future, as the quality of the current data set is unclear. It is recommended to combine the point measurements of bed-material samples with synoptic views of bed sediment composition patterns derived from multibeam echosounder backscatter (Eleftherakis *et al.*, 2010; Kinneging *et al.*, 2012; Eleftherakis, 2013). For the subsurface, an underlayer model based on geological data could provide us with further understanding of how the river was built up in the past. We recommend to review the existing information on underlayers from Gruijters *et al.* (2001), and if still sufficiently accurate use this to analyse the model behaviour. Interesting to mention regarding the characterisation of the subsurface is the application of sub-bottom profilers and side scan sonar (pers. communication Ane Wiersma).

With regards to the stability of the river bed we recommend to study the influence of coarseness of nourishments on the response to the river bed. This is linked to the modelling of this behaviour for which recommendations were given above. Besides this, it is recommended to look into smart dredging, i.e. find where coarse material resides in shallow areas and nourish these at degrading parts of the river.

8.2 Modelling of armoured layers

It is not clear which physical processes of interest for Rijkswaterstaat cannot be modelled using the active-layer model. We suggest to clarify the limitation of the current modelling strategy clearly identifying what are the current caveats and what are the desired functionalities and capabilities.

We suggest to further study and verify the capabilities of the active-layer model in reproducing the cases that were previously thought not possible to model (i.e., a case similar to the experiment conducted by Struiksma (1999) with mixed-size sediment, i.e. one mobile and one immobile fraction). This will require considering the following questions:

1 What are the limitations of using the active-layer model in the presence of an armour layer?
2 On which parameters is the active-layer thickness dependent?
3 How can we predict the sediment transport rate under conditions in which the sediment in the active layer is partially mobile?

4 What are the limitations of using a standard function for accounting for the hiding effect (e.g., Egiazaroff (1965))?
5 How should we model the flux of sediment between the active layer and the substrate?
6 What is the additional benefit of considering a grain-size-dependent sediment flux (such as included in the code of (Tuijnder *et al.*, 2011))?

Gabrielle Massera, a student from the University of Trento, has started working on his research to further identify the problems to the modelling concepts of graded sediment in the case of armoured layers. The findings of his study should provide more insight into the modelling of armoured layers, and once a concept has been proven within a simple research code, it could also be included inside Delft3D.

References

Blom, A., J. S. Ribberink and H. J. de Vriend, 2003. "Vertical sorting in bed forms: Flume experiments with a natural and a trimodal sediment mixture." *Water Resour. Res.* 39 (2): 1025. DOI: 10.1029/2001WR001088, ISSN 1944-7973, URL http://dx.doi.org/10.1029/2001WR001088.

ten Brinke, W. B. M., 2005. *The Dutch Rhine: A restrained river*. Veen Magazines, Amsterdam, the Netherlands.

Colombini, M., 2004. "Revisiting the linear theory of sand dune formation." *J. Fluid Mech.* 502: 1–16. DOI: 10.1017/S0022112003007201, ISSN 1469-7645, URL http://journals.cambridge.org/article_S0022112003007201.

Colombini, M. and A. Stocchino, 2005. "Coupling or decoupling bed and flow dynamics: Fast and slow sediment waves at high Froude numbers." *Phys. Fluids* 17 (3): 036602. DOI: 10.1063/1.1848731, URL http://dx.doi.org/10.1063/1.1848731.

Deltares, 2013. *Delft3D-FLOW, User Manual*. Rotterdamseweg 185, p.o. box 177, 2600 MH Delft, The Netherlands, 3.15.30059 ed.

Egiazaroff, I. V., 1965. "Calculation of nonuniform sediment concentrations." *J. Hydraulics Div.* 91 (4): 225–247.

Einstein, H. A., 1950. *The bed-load function for sediment transportation in open channel flows*. Tech. Bull. 1026, US Department of Agriculture, Soil Conservation Service, Washington, DC, United States.

Eleftherakis, D., 2013. *Classifying sediments on Dutch riverbeds using multi-beam echo-sounder systems*. Ph.D. thesis.

Eleftherakis, D., E. Mosselman, A. Amiri-Simkooei, S. Giri, M. Snellen and D. Simons, 2010. "Identifying changes in river bed morphology and bed sediment composition using multi-beam echo-sounder measurements." In *Proc. 10th European Conf. Underwater Acoustics, Istanbul, Turkey, July 5–9*, vol. 2, pages 1365–1373.

Exner, F. M., 1920. "Zur Physik der Dünen." *Akad. Wiss. Wien Math. Naturwiss* 129 (2a): 929–952. (in German).

Gruijters, S., J. Veldkamp, J. Gunnink and J. Bosch, 2001. *The lithological and sedimentological structure of the Pannerdensche Kop bifurcation*. Tech. rep., Geological Survey of the Netherlands (TNO).

Hirano, M., 1971. "River bed degradation with armoring." *Proc. Jpn. Soc. Civ. Eng.* 195: 55–65. DOI: 10.2208/jscej1969.1971.195_55.

Kinneging, N., M. Snellen, D. Eleftherakis, D. Simons, E. Mosselman and A. Sieben, 2012. "River bed classification using multi-beam echo-sounder backscatter data." In T. A. G. P. van Dijk, ed., *Proc. Hydro12 - Taking care of the sea, Rotterdam, the Netherlands, 13–15 November*. Hydrographic Society Benelux.

Koch, F. G. and C. Flokstra, 1980. *Bed level computations for curved alluvial channels*. Tech. Rep. 240, Delft Hydraulics Laboratory, Delft, the Netherlands.

Luu, X. L., H. Takebayashi and S. Egashira, 2004. "Characteristics of sediment sorting predicted by two different exchange layer models." *Jap. Soc. Fluid Mech.* A225: 248–249.

Meyer-Peter, E. and R. Müller, 1948. "Formulas for bed-load transport." In *Proc. 2nd IAHR World Congress, 6–9 June, Stockholm, Sweden*, pages 39–64.

Niesten, I., W. Ottevanger and A. Becker, 2017. *Riviersuppleties in de Rijntakken*. Tech. rep., Deltares, Delft, the Netherlands.

Omer, A., 2019. *Modelling the morphological effects of longitudinal dams in the Midden-Waal*. Tech. Rep. 11203681-002-ZWS-0001, Deltares, Delft, the Netherlands.

Ottevanger, W., 2015. *Operationeel maken invloed semi-harde lagen in splitsingspuntengebied*. Tech. Rep. 1220038-005, Deltares, Delft, the Netherlands.

Ottevanger, W., 2017. *Kwaliteit berekende statistiek : Waal bodemligging en minimale diepte*. Tech. Rep. 1230041-011-ZWS-0001, Deltares, Delft, the Netherlands.

Ottevanger, W., S. Giri and K. Sloff, 2015. *Sustainable Fairway Rhinedelta II*. Tech. Rep. 1209175-000, Deltares, Delft, the Netherlands.

Paola, C. and R. Seal, 1995. "Grain Size Patchiness as a Cause of Selective Deposition and Downstream Fining." *Water Resour. Res.* 31 (5): 1395–1407. DOI: 10.1029/94WR02975, URL https://agupubs.onlinelibrary.wiley.com/doi/abs/10.1029/94WR02975.

Ribberink, J. S., 1987. *Mathematical modelling of one-dimensional morphological changes in rivers with non-uniform sediment*. Ph.D. thesis, Delft University of Technology, Delft, the Netherlands.

van Rijn, L. C., 1984. "Sediment Transport, Part I: Bed Load Transport." *J. Hydraul. Eng.* 110 (10): 1431–1456. DOI: 10.1061/(ASCE)0733-9429(1984)110:10(1431).

Scheffer, M., S. R. Carpenter, T. M. Lenton, J. Bascompte, W. Brock, V. Dakos, J. van de Koppel, I. A. van de Leemput, S. A. Levin, E. H. van Nes, M. Pascual and J. Vandermeer, 2012. "Anticipating Critical Transitions." *Science* 338 (6105): 344–348. DOI: 10.1126/science.1225244, ISSN 0036-8075, URL https://science.sciencemag.org/content/338/6105/344.

Shields, A., 1936. *Anwendung der Ähnlichkeitsmechanik und Turbulenzforschung auf die Geschiebebewegung*. Ph.D. thesis, Versuchsanstalt für Wasserbau und Schiffbau, 26, Berlin, Germany. (in German).

Struiksma, N., 1999. "Mathematical modelling of bedload transport over non-erodible layers." In *Proceedings of the 1st IAHR symposium on River, Coastal, and Estuarine Morphoynamics, Genova, Italy*, pages 89–98.

Tuijnder, A. and J. Ribberink, 2010a. *A morphological concept for semi-fixed layers*. Tech. Rep. 2011R-003/WEM-003, Twente University, Enschede, the Netherlands.

Tuijnder, A., J. Ribberink and A. Spruijt, 2011. *Modelling semi-fixed layers with Delft3D*. Tech. Rep. 2011R-004/WEM-004, Twente University, Enschede, the Netherlands.

Tuijnder, A. and J. S. Ribberink, 2010b. "Development of supply-limited transport due to vertical sorting of a sand-gravel mixture." In R. M. M. noz, ed., *Proceedings of the international conference on fluvial hydraulics (River Flow), Braunschweig, Germany, 8-10 September*, pages 487–492. CRC press, Taylor and Francis Group.

Tuijnder, A. and J. S. Ribberink, 2012. "Immobile layer formation due to vertical sorting of immobile grain size fractions." In K. Koll, A. Dittrich, J. Aberle and P. Geisenhainer, eds., *Proceedings of the international conference on fluvial hydraulics (River Flow), San José, Costa Rica, 5-7 September*, pages 847–854. Bundesanstalt für Wasserbau, Karlsruhe, Germany.

Tuijnder, A., A. Spruijt and J. Ribberink, 2012. *Application of the Delft3D semi-fixed layer model to Boven-Rijn and Pannerdensch Kanaal*. Tech. Rep. 2012R-0xx/WEM-0xx, Twente University, Enschede, the Netherlands.

Wang, Z., M. D. Vries, R. Fokkink and A. Langerak, 1995. "Stability of river bifurcations in ID morphodynamic models." *J. Hydraul. Res.* 33 (6): 739–750. DOI: 10.1080/00221689509498549.

Wilcock, P. R. and B. W. McArdell, 1997. "Partial transport of a sand/gravel sediment." *Water Resour. Res.* 33 (1): 235–245. DOI: 10.1029/96WR02672, ISSN 1944-7973, URL http://dx.doi.org/10.1029/96WR02672.

Wu, F. and K. Yang, 2004. "Entrainment Probabilities of Mixed-Size Sediment Incorporating Near-Bed Coherent Flow Structures." *J. Hydraul. Eng.* 130 (12): 1187–1197. DOI: 10.1061/(ASCE)0733-9429(2004)130:12(1187), URL http://ascelibrary.org/doi/abs/10.1061/%28ASCE%290733-9429%282004%29130%3A12%281187%29.

Yossef, M. F., H. Jagers, S. van Vuren and A. Sieben, 2008. "Innovative techniques in modelling large-scale river morphology." In M. Altinakar, M. A. Kokpinar, İsmail Aydin, Şevket Cokgor and S. Kirgoz, eds., *Procedings of the 4th International Conference on Fluvial Hydraulics (River Flow), 3-5 September, Cesme, Izmir, Turkey*. Kubaba Congress Department and Travel Services, Ankara, Turkey.

A Results of the simple testcases

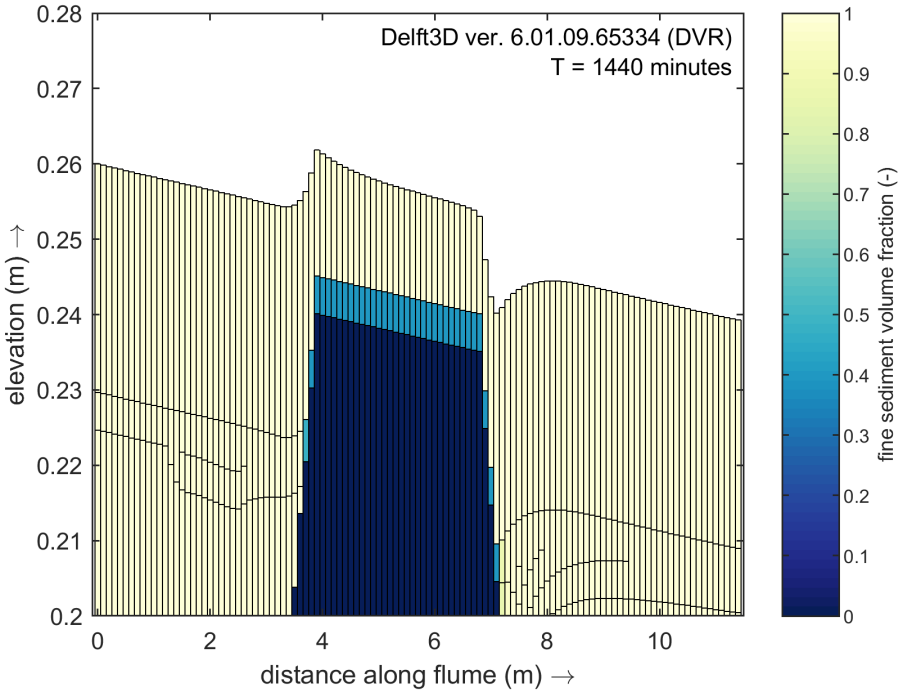

Figure A.1: *Final sediment volume fraction in the bed for case C2*

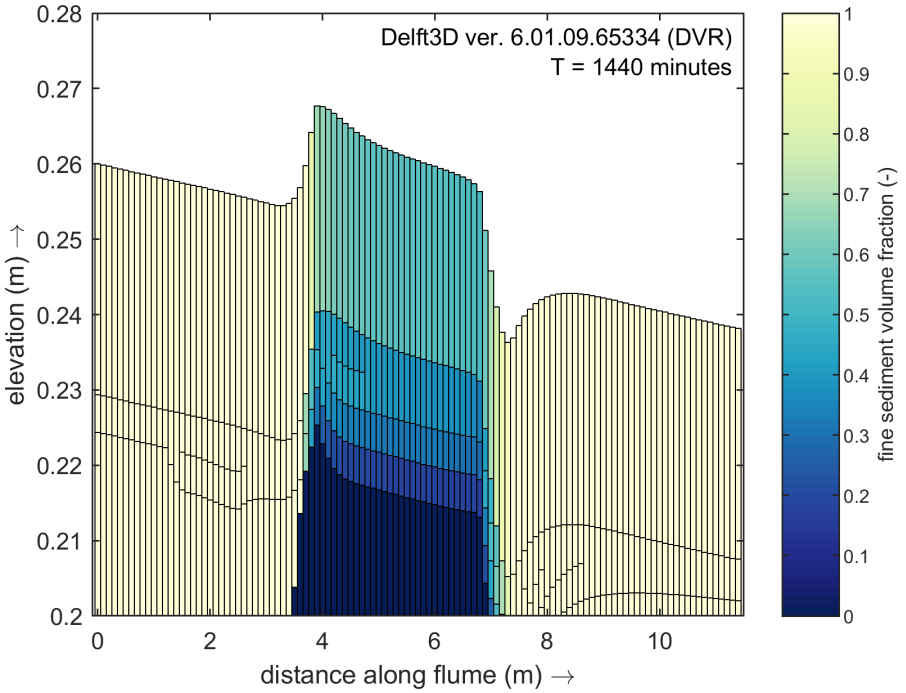

Figure A.2: *Final sediment volume fraction in the bed for case C3*

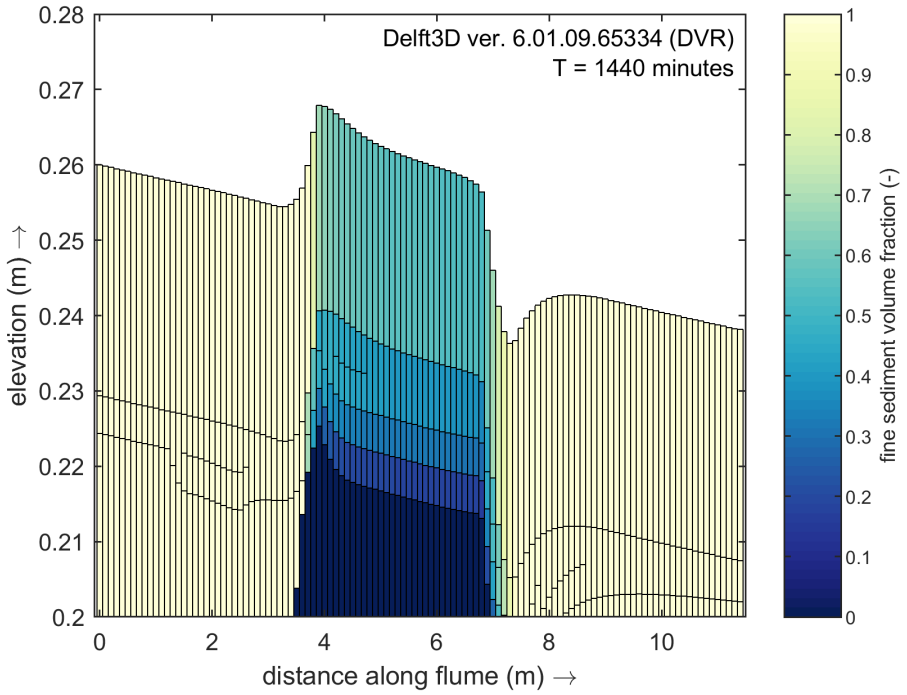

Figure A.3: *Final sediment volume fraction in the bed for case C4*

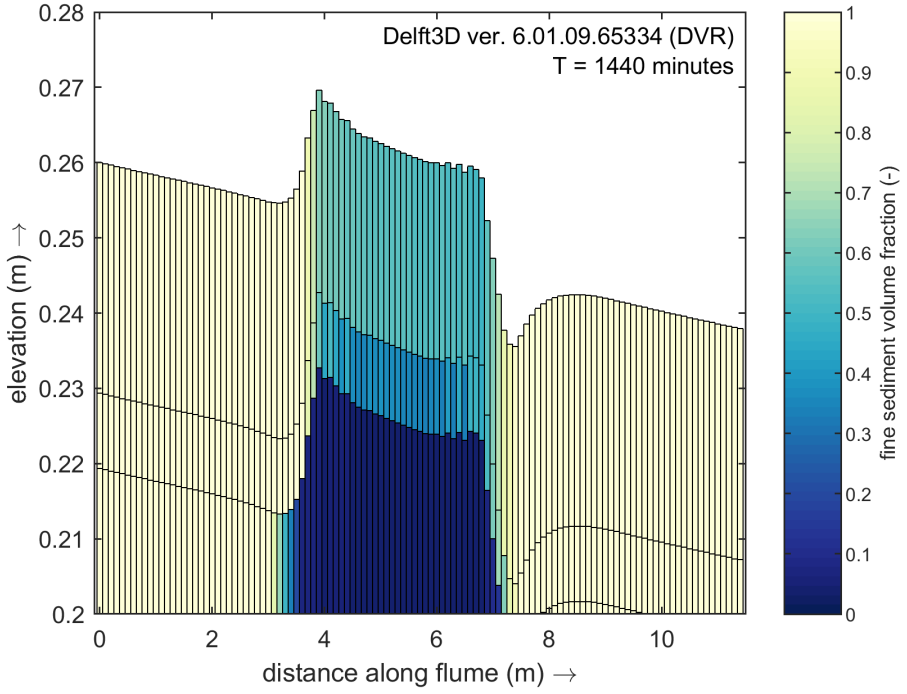

Figure A.4: *Final sediment volume fraction in the bed for case C5*

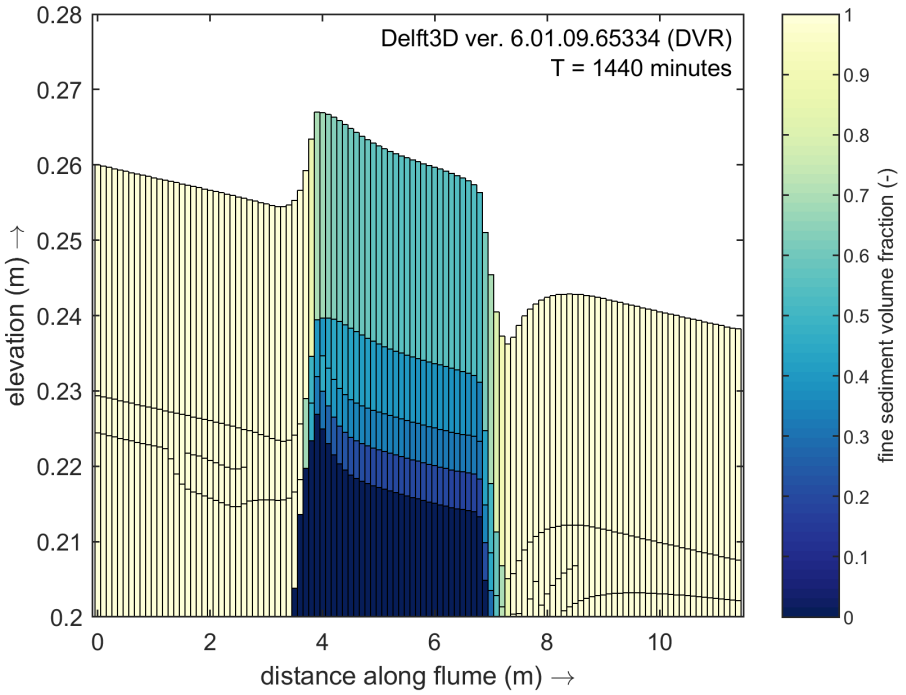

Figure A.5: *Final sediment volume fraction in the bed for case C6*

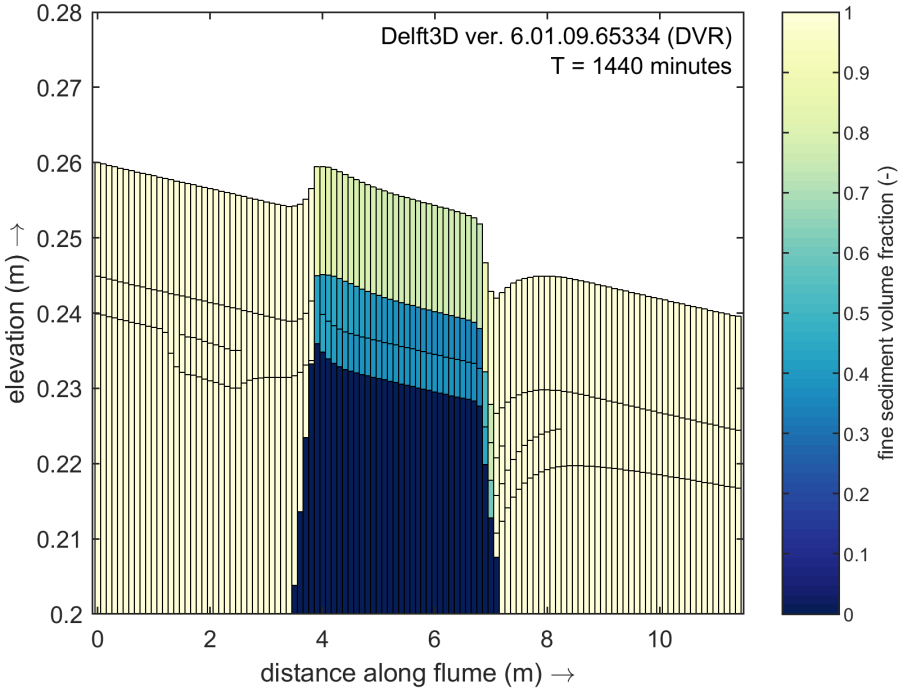

Figure A.6: *Final sediment volume fraction in the bed for case C7*